2. Materials and methods

2.1. Antibodies

Polyclonal antibodies were raised against synthetic peptides corresponding to residues 1–10, 11–20, 21–30, 31–40, 41–50, 51–60, 61–70, 75–91 and 131–140 of human α-synuclein, with Cys at the C-terminus or the N-terminus (Greiner Bio-One Co. Ltd.) (Table 1). The peptides were conjugated to *m*-maleimidobenzoyl-*N*-hydrosuccinimide ester-activated keyhole limpet hemocyanin (KLH). The KLH-peptide complex (1 mg of each immunogen) emulsified in Freund's complete adjuvant was injected subcutaneously into a New Zealand White rabbit, followed by 5 weekly subcutaneous injections of 150 μg KLH-peptide complex emulsified in Freund's incomplete adjuvant, starting 3 weeks after the first immunization. Antibody Syn259, which recognizes residues 104–119 of α-synuclein, was kindly provided by Dr. S. Nakajo.

2.2. Expression and purification of α-synuclein

Human α-synuclein was expressed in *E. coli* BL21 (DE3) cells, as described [9]. To avoid the production of α-synuclein dimers induced by misexpression of cysteine-containing α-synuclein, the Y136-TAT construct was used [12]. α-Synuclein was purified by boiling, Q-Sepharose ion exchange chromatography and ammonium sulfate precipitation, followed by dialysis against 30 mM Tris–HCl, pH 7.5, and the determination of protein concentrations, as described [9].

2.3. Preparation of α-synuclein fibrils and inhibitor-bound monomers and dimers

Purified α-synuclein (7 mg/ml) was incubated at 37 °C in a shaking incubator (200 rpm) in 30 mM Tris–HCl, pH 7.5, containing 0.1% NaN_3, for 72 h. Fibrils were pelleted by spinning the assembly mixtures at 113000×*g* for 20 min. To prepare SDS-stable, inhibitor-bound monomers and dimers, the polyphenol exifone was used in most experiments [9]. Similar results were obtained with dopamine and gossypetin, two previously described inhibitory compounds [4,9]. Exifone-bound α-synuclein monomers (Exi-monomer) and dimers (Exi-dimer) were prepared by gel filtration, as described [9]. Briefly, α-synuclein (7 mg/ml) was incubated in the presence of 2 mM inhibitory compound at 37 °C for 72 h in 30 mM Tris-HCl containing 0.1% sodium azide, and centrifuged at 113000×*g* for 20 min. The supernatants were loaded onto a Superdex 200 gel filtration column (1 × 30 cm), eluted in 10 mM Tris–HCl, pH 7.5, containing 150 mM NaCl, and monitored at 214 nm. Fractionated samples were analyzed by SDS–PAGE and immunoblotting. Protein concentrations were determined as described [9].

Table 1
Antigen peptides for immunization of rabbits.

Name of antibodies	AA residues	Antigen peptide
Syn1-10	1–10	MDVFMKGLSKC
Syn11-20	11–20	AKEGVVAAAEC
Syn21-30	21–30	KTKQGVAEAAC
Syn31-40	31–40	GKTKEGVLYVC
Syn41-50	41–50	GSKTKEGVVHC
Syn51-60	51–60	GVATVAEKTKC
Syn61-70	61–70	EQVTNVGGAVC
Syn75-91	75–91	CTAVAQKTVEGAGSIAAA
Syn131-140	131–140	CEGYQDYEPEA

2.4. ELISA and dot blot assay

For the ELISA, peptide immunogens, α-synuclein monomers and fibrils, as well as Exi-monomers and dimers (0.5–1.0 μg/well in 50 mM Tris–HCl, pH 8.8) were coated onto microtitre plates (SUMILON) at 4 °C for 16 h. The plates were blocked with 10% fetal bovine serum (FBS) in PBS, incubated with the first antibody diluted in 10% FBS/PBS at room temperature for 1.5 h, followed by incubation with HRP-goat anti-rabbit IgG (Bio-Rad) at 1:1000 dilution, and reacted with the substrate, 0.4 mg/ml *o*-phenylendiamine, in citrate buffer (24 mM citric acid, 51 mM Na_2HPO_4). The absorbance at 490 nm was measured using Plate Chameleon (HIDEX). For the dot blot assay, 100 ng α-synuclein was spotted onto a PVDF membrane by using a dot blot apparatus (Bio-Rad). Membranes were stained with Coomassie Brilliant Blue or blocked with 3% gelatin/PBS and incubated overnight at room temperature with anti-α-synuclein antibodies in 10% FBS/PBS. Immunoreactivity was detected with avidin-biotin (Vector Laboratories) and developed using NiCl-enhanced diaminobenzidine. The rate of reactivity was quantified by scanning densitometry and expressed relative to the density of α-synuclein fibrils (taken as 100%).

3. Results

3.1. Antibody specificities

In order to detect conformational changes in α-synuclein, antibodies were raised against nine peptides (corresponding to residues 1–10, 11–20, 21–30, 31–40, 41–50, 51–60, 61–70, 75–91 and 131–140) (Table 1). The specificities of the antibodies were analyzed by ELISA. The peptides used as immunogens were coated on a plate and probed with each antibody. As shown in Fig. 1, each antibody reacted strongly with the appropriate peptide, but hardly with the other peptides. Antibody Syn41–50 was an exception, in that it weakly recognized peptides 11–20 and 31–40, in addition to recognizing peptide 41–50 very strongly.

3.2. Analysis of conformational changes in α-synuclein using epitope-specific antibodies

We investigated the reactivity of monomeric α-synuclein and of α-synuclein fibrils by dot blot assay using the nine antibodies described above and antibody Syn259 whose epitope corresponds to residues 104–119 of α-synuclein. Monomeric α-synuclein was strongly detected by antibodies to the C-terminal region (Syn259 and Syn131–140), but not by antibodies to the N-terminal or middle region (Fig. 2). This is in good agreement with previous reports showing that the C-terminal region of α-synuclein is unfolded and shields the N-terminal and central regions by way of long-range intramolecular interactions [13,14]. In contrast, α-synuclein fibrils were strongly immunoreactive with all antibodies (Fig. 2), indicating that the relevant epitopes were accessible. This is also consistent with current knowledge of the location of individual β-strands and their connecting loops in the structure of the α -synuclein fibril [15,16]. These results indicate that conformational changes undergone by α-synuclein as it assembles into fibrils can be detected immunochemically. We next analyzed the conformations of exifone-stabilized monomers and dimers of α-synuclein, following their separation by gel filtration chromatography (Supplementary Fig.). SDS-stable dimers formed in the presence of exifone were recognized by antibodies specific for Syn1–10, Syn11–20, Syn21–30, Syn31–40 and Syn41–50 (Fig. 2). They were less well recognized by antibodies specific for Syn51–60, Syn61–70 and Syn75–91. The antibody recognition patterns of SDS-stable monomers formed in the presence of exifone were intermediate between

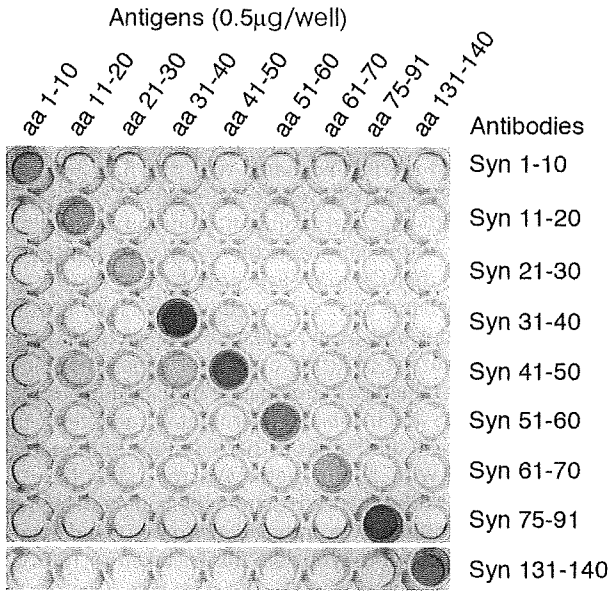

Fig. 1. Specificities of anti-peptide antibodies spanning the whole of α-synuclein determined by ELISA. Synthetic peptides (0.5 µg/well) were coated on a 96-well microtitre plate for 16 h at 4 °C and each of the 9 peptides was probed with each of the 9 antisera.

those of untreated monomers and polyphenol-stabilized dimers (Fig. 2). All antibodies gave similar results by ELISA (data not shown).

4. Discussion

We show here that the conformational changes undergone by α-synuclein during the conversion from monomers to amyloid fibrils can be detected by epitope-specific antibodies. Antibodies to the C-terminal region of α-synuclein recognized monomers and fibrils almost equally, whereas antibodies to the N-terminal region strongly reacted with fibrils, but labelled monomers only weakly. Under physiological conditions, α-synuclein is known to populate an ensemble of conformations, including conformers that are more compact than expected for a random coil protein [17–19]. Our findings indicating that the N-terminal region is buried and only poorly accessible to antibodies, are in line with this work. They are also in agreement with reports showing that the C-terminal region of α-synuclein is unfolded and shields the N-terminal and central regions by way of long-range intramolecular interactions [13,14].

The core of the fibril spans approximately residues 30–100 of α-synuclein [20,21] and is believed to comprise five parallel β-strands that are separated by flexible loops [16]. Our findings on α-synuclein fibrils are consistent with the loop regions being antibody-accessible. Conformational changes detectable by specific antibodies have previously been reported in tau, another natively unfolded protein, as it assembles into abnormal filaments. Thus, antibody Alz50 reacts more strongly with paired helical filament tau from Alzheimer's disease brain than with the soluble monomeric protein [22].

Inhibitor-bound dimers and monomers of α-synuclein were tested using the same panel of antibodies. When bound to the polyphenol exifone, dimers of α-synuclein were detected by antibodies to the N-terminal region in a manner similar to fibrils. Unlike the latter, inhibitor-bound dimers were not recognized by antibodies to the middle region of α-synuclein. Antibodies to the C-terminal region recognized inhibitor-bound dimers and fibrils equally. Relative to unbound monomers, therefore, inhibitor-bound α-synuclein dimers are characterized by a more accessible N-terminal region. NMR spectroscopy of exifone-stabilized α-synuclein dimers and nitroblue tetrazolium staining of cleaved exifone-bound α-

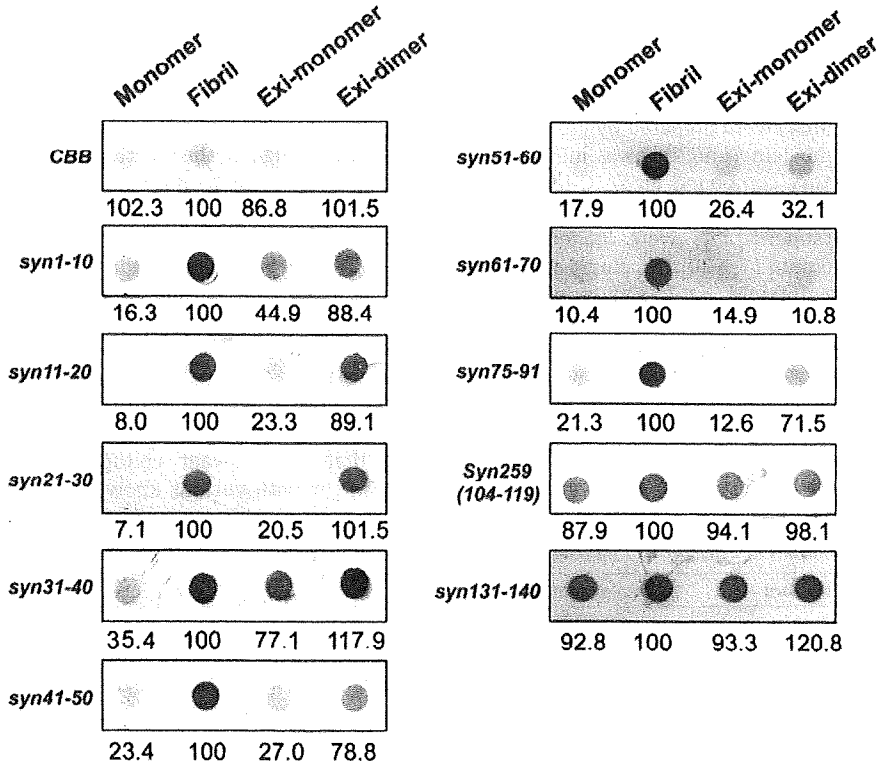

Fig. 2. Dot blot analysis of monomeric α-synuclein, the α-synuclein fibril, as well as exifone-stabilized α-synuclein monomers (Exi-monomer) and dimers (Exi-dimer), with 10 antibodies whose epitopes span the whole of human α-synuclein. The relative intensities of immunoreactivity are indicated below the dots and expressed as % of fibril immunoreactivity (taken as 100, $n = 3$). Each dot corresponds o 100 ng of α-synuclein.

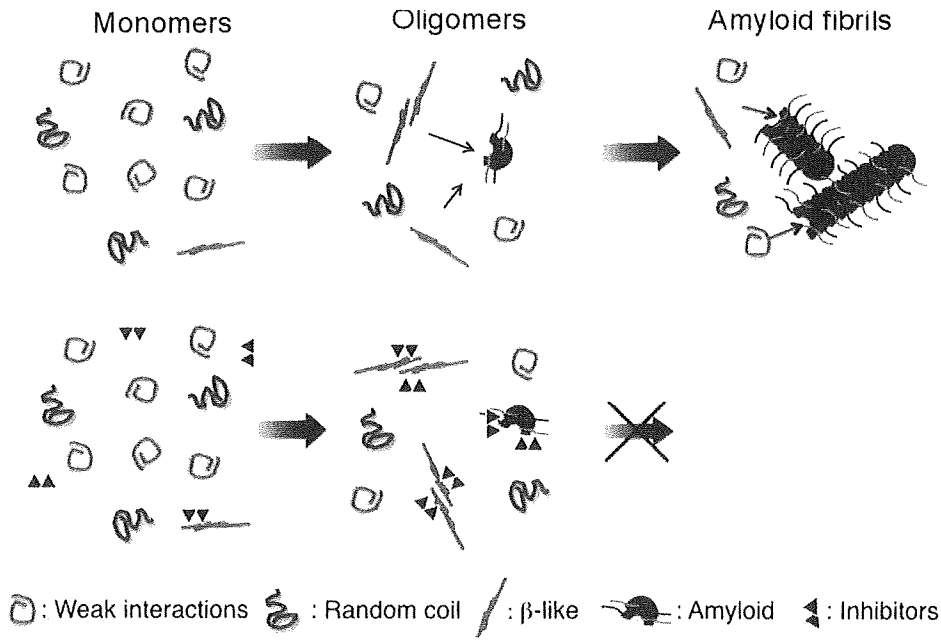

Fig. 3. Model of the inhibition of α-synuclein fibril formation by small molecules.

synuclein showed that N-terminal regions are involved in dimer formation and that exifone binds to these regions (in preparation). Dimers of α-synuclein are believed to play a key role in the aggregation process [23]. A recent study has also shown that aggregation-inhibiting molecules interact with N-terminal regions of α-synuclein [24]. When tested with the panel of antibodies, inhibitor-bound monomers of α-synuclein gave a pattern intermediate between that of unbound monomers and inhibitor-bound dimers. Taken together, our findings suggest the existence of a linear pathway leading from monomeric to fibrillar α-synuclein, with exifone binding to misfolded monomers and dimers, thereby preventing fibril formation. A similar mechanism may underlie the inhibition of α-synuclein fibril formation by the molecular chaperone Hsp70 [25].

This interpretation is at odds with a recent study reporting that oligomers of α-synuclein and Aβ formed in the presence of EGCG were off-pathway [11]. In this study, conformation-specific antibody A11, which recognizes an oligomeric state that is believed to be common to many amyloidogenic proteins [26], did not detect EGCG-induced oligomers. This antibody is believed to be specific for on-pathway toxic oligomers of α-synuclein. However, Ehrnhoefer et al. found that it recognized His-tagged monomeric α-synuclein [11]. In our hands, antibody A11 also recognized α-synuclein fibrils (unpublished observation).

Single molecule studies have shown that α-synuclein exists as three distinct conformers *in vitro* that are characterized by: long-distance weak interactions, random coil and β-like structures [27]. The β-like conformer has been linked to the process of α-synuclein aggregation. It is tempting to suggest that exifone binds to this conformer, in line with the finding that inhibitory compounds inhibit amyloid fibril formation at substoichiometric concentrations [8,9]. Our previous work on the ordered aggregation of tau protein has also shown that small molecule inhibitors bind to oligomers and filaments, but not to native monomers [8]. A revised model for the inhibition of α-synuclein fibril formation by small molecules is shown in Fig. 3. Monomeric α-synuclein exists in a native conformation, with a small proportion of β-like structure. During assembly, the latter may dimerize, oligomerize and form amyloid seeds. Amyloid fibrils can grow from these seeds. Small molecule inhibitors bind to misfolded monomers, dimers and oligomers, thus preventing fibril formation.

Acknowledgements

This work was supported by a Grant-in-aid for Scientific Research on Priority Areas – Research on Pathomechanisms of Brain Disorders (to M.H., 20023038) and Grants-in-aid for Scientific Research (B) (to M.H., 18300117) and (C) (to T.N.) from the Ministry of Education, Culture, Sports, Science and Technology of Japan.

Appendix A. Supplementary data

Supplementary data associated with this article can be found, in the online version, at doi:10.1016/j.febslet.2009.01.037.

References

[1] Goedert, M. and Spillantini, M.G. (2006) A century of Alzheimer's disease. Science 314, 777–781.
[2] Goedert, M. (2001) α-Synuclein and neurodegenerative diseases. Nature Rev. Neurosci. 2, 492–501.
[3] Findeis, M.A. (2000) Approaches to discovery and characterization of inhibitors of amyloid β-peptide polymerization. Biochim. Biophys. Acta 1502, 76–84.
[4] Conway, K.A., Rochet, J.C., Bieganski, R.M. and Lansbury, P.T. (2001) Kinetic stabilization of the α-synuclein protofibril by a dopamine-α-synuclein adduct. Science 294, 1346–1349.
[5] Heiser, V., Engemann, S., Bröcker, W., Dunkel, I., Boeddrich, A., Waelter, S., Nordhoff, E., Lurz, R., Schugardt, N., Rautenberg, S., Herhaus, C., Barnickel, G., Böttcher, H., Lehrach, H. and Wanker, E.E. (2002) Identification of benzothiazoles as potential polyglutamine aggregation inhibitors of Huntington's disease by using an automated filter retardation assay. Proc. Natl. Acad. Sci. USA 99, 16400–16406.
[6] Cashman, N.R. and Caughey, B. (2004) Prion diseases: close to effective therapy? Nat. Rev. Drug Discov. 3, 874–884.
[7] Pickhardt, M., Gazova, Z., von Bergen, M., Khlistunova, I., Wang, Y., Hascher, A., Mandelkow, E.M., Biernat, J. and Mandelkow, E. (2005) Anthraquinones inhibit tau aggregation and dissolve Alzheimer's paired helical filaments *in vitro* and in cells. J. Biol. Chem. 280, 3628–3635.
[8] Taniguchi, S., Suzuki, N., Masuda, M., Hisanaga, S., Iwatsubo, T., Goedert, M. and Hasegawa, M. (2005) Inhibition of heparin-induced tau filament formation by phenothiazines, polyphenols, and porphyrins. J. Biol. Chem. 280, 7614–7623.

[9] Masuda, M., Suzuki, N., Taniguchi, S., Oikawa, T., Nonaka, T., Iwatsubo, T., Hisanaga, S.-I., Goedert, M. and Hasegawa, M. (2006) Small molecule inhibitors of α-synuclein filament assembly. Biochemistry 45, 6085–6094.
[10] Hong, D.-P., Fink, A.L. and Uversky, V.N. (2008) Structural characteristics of α-synuclein oligomers stabilized by the flavonoid baicalein. J. Mol. Biol. 383, 214–223.
[11] Ehrnhoefer, D.E., Bieschke, J., Boeddrich, A., Herbst, M., Masino, L., Lurz, R., Engemann, S., Pastore, A. and Wanker, E.E. (2008) EGCG redirects amyloidogenic polypeptides into unstructured, off-pathway oligomers. Nat. Struct. Mol. Biol. 15, 558–566.
[12] Masuda, M., Dohmae, N., Nonaka, T., Oikawa, T., Hisanaga, S.-I., Goedert, M. and Hasegawa, M. (2006) Cysteine misincorporation in bacterially expressed human α-synuclein. FEBS Lett. 580, 1775–1779.
[13] Dedmon, M.M., Lindorff-Larsen, K., Christodoulou, J., Vendruscolo, M. and Dobson, C.M. (2005) Mapping long-range interactions in α-synuclein using spin-label NMR and ensemble molecular dynamics simulations. J. Am. Chem. Soc. 127, 476–477.
[14] Bertoncini, C.W., Jung, Y.S., Fernandez, C.O., Hoyer, W., Griesinger, C., Jovin, T.M. and Zweckstetter, M. (2005) Release of long-range tertiary interactions potentiates aggregation of natively unstructured α-synuclein. Proc. Natl. Acad. Sci. USA 102, 1430–1435.
[15] Heise, H., Hoyer, W., Becker, S., Andronesi, O.C., Riedel, D. and Baldus, M. (2005) Molecular-level secondary structure, polymorphism, and dynamics of full-length α-synuclein fibrils studied by solid-state NMR. Proc. Natl. Acad. Sci. USA 102, 15871–15876.
[16] Vilar, M., Chou, H.-T., Lührs, T., Maji, S.K., Riek-Loher, D., Verel, R., Manning, G., Stahlberg, H. and Riek, R. (2008) The fold of α-synuclein fibrils. Proc. Natl. Acad. Sci. USA 105, 8637–8642.
[17] Syme, C.D., Blanch, E.W., Holt, C., Jakes, R., Goedert, M., Hecht, L. and Barron, L.D. (2001) A Raman optical activity study of rheomorphism in caseins, synucleins and tau: New insight into the structure and behaviour of natively unfolded proteins. Eur. J. Biochem. 269, 148–156.
[18] Maiti, N.C., Apetrui, M.M., Zagorski, M.G., Carey, P.R. and Anderson, V.R. (2004) Raman spectroscopic characterization of secondary structure in natively unfolded proteins: α-Synuclein. J. Am. Chem. Soc. 126, 2399–2408.
[19] Lee, J.C., Langen, R., Hummal, P.A., Gray, H.B. and Winkler, J.R. (2004) α-Synuclein structures from fluorescence energy-transfer kinetics: Implications for the role of the protein in Parkinson's disease. Proc. Natl. Acad. Sci. USA 101, 16466–16471.
[20] Miake, H., Mizusawa, H., Iwatsubo, T. and Hasegawa, M. (2002) Biochemical characterization of the core structure of α-synuclein filaments. J. Biol. Chem. 277, 19213–19219.
[21] Der-Sarkissian, A., Jao, C.C., Chen, J. and Langen, R. (2003) Structural organization of α-synuclein fibril structure studied by site-directed spin labeling. J. Biol. Chem. 278, 24970–24979.
[22] Carmel, G., Mager, E.M., Binder, L.I. and Kuret, J. (1996) The structural basis of monoclonal antibody Alz50's selectivity for Alzheimer's disease pathology. J. Biol. Chem. 271, 32789–32795.
[23] Yu, J., Malkova, S. and Lyubchenko, Y.L. (2008) α-Synuclein misfolding: single molecule AFM force spectroscopy study. J. Mol. Biol. 384, 992–1001.
[24] Rao, J.N., Dua, V. and Ulmer, T.S. (2008) Characterization of α-synuclein interactions with selected aggregation-inhibiting small molecules. Biochemistry 47, 4651–4656.
[25] Luk, K.C., Mills, I.P., Trojanowski, J.Q. and Lee, V.M.-Y. (2008) Interactions between Hsp70 and the hydrophobic core of α-synuclein inhibit fibril assembly. Biochemistry 47, 12614–12625.
[26] Kayed, R., Head, E., Thompson, J.L., McIntire, T.M., Milton, S.C., Cotman, C.W. and Glabe, C.G. (2003) Common structure of soluble amyloid oligomers implies common mechanism of pathogenesis. Science 300, 486–489.
[27] Sandal, M., Valle, F., Tessari, I., Mammi, S., Bergantino, E., Musiani, F., Brucale, M., Bubacco, L. and Samori, B. (2008) Conformational equilibria in monomeric α-synuclein at the single-molecule level. PLoS Biol. 6, e6.

DNA AND CELL BIOLOGY
Volume 28, Number 12, 2009

Pp. 625–631
DOI: 10.1089/dna.2009.0877

Involvement of NAD(P)H:Quinone Oxidoreductase 1 and Superoxide Dismutase Polymorphisms in Ulcerative Colitis

Toshihito Kosaka,[1] Junji Yoshino,[1] Kazuo Inui,[1] Takao Wakabayashi,[1] Takashi Kobayashi,[1] Shinya Watanabe,[1] Shigekazu Hayashi,[2] Yoshifumi Hirokawa,[3] Taizo Shiraishi,[3] Takayuki Yamamoto,[4] Mayumi Tsuji,[5] Takahiko Katoh,[5] and Masatoshi Watanabe[6]

Inflammatory bowel disease is a multifactorial disease. Oxidative stress has been thought to be one of etiologic factor for inflammatory bowel disease. The genes superoxide dismutase (*SOD2*) and NAD(P)H:quinone oxidoreductase 1 (*NQO1*) are involved in inflammation and oxidative stress. The purpose of the present case–control study with 134 patients with ulcerative colitis (UC) and 125 healthy controls was to determine whether polymorphisms of these genes, the *NQO1* C609T and the *SOD2* Ala-9Val, are associated with the risk of UC and influence the clinical characteristics. These polymorphisms were examined by polymerase chain reaction–restriction fragment length polymorphisms and direct sequencing. In patients showing steroid resistance, the number with the *NQO1* T/T genotype was significantly higher than other genotypes (odds ratio 9.45, 95% confidence interval 2.46–41.6, $p = 0.002$). In the patients whose onset of UC was age 20 years or younger, more patients had *SOD2* T/T genotype than the other genotypes (odds ratio 6.46, 95% confidence interval 0.82–51.0). No association between these polymorphisms and UC risk was apparent. The *NQO1* C609T polymorphism may influence steroid resistance of UC patients, while the *SOD2* Ala-9Val polymorphism may influence age of onset of UC. Oxidative stress may influence the clinical features of UC.

Introduction

INFLAMMATORY BOWEL DISEASE (IBD) includes two common forms, Crohn's disease (CD) and ulcerative colitis (UC), and is recognized as a multifactorial disease (Koutroubakis *et al.*, 1996). Factors that may affect IBD include diet, infantile environment, and immune defense abnormalities limited to the intestinal tract. Recently, oxidative stress has been proposed to be a factor that influences IBD (Kruidenier *et al.*, 2003). Koutroubakis *et al.* (2004) showed that serum total antioxidant capacity was lower in both CD and UC patients compared with healthy controls. This finding suggests that decreased antioxidant defenses may be a primary phenomenon severely compromising the mucosa and increasing its susceptibility to oxidative tissue damage. Genetic factors have also been examined in IBD, but despite the many studies that have searched for susceptibility genes to IBD, there is currently no consensus (Orchard *et al.*, 2000). However, a recent genome-wide study for UC susceptibility genes was performed in 1052 individuals with UC (Silverberg *et al.*, 2009). In this study, UC loci attaining genome-wide significance levels were identified on chromosome 1p36 and 12q15. In this current study, we investigated the effect of NADP(H):quinone oxidoreductase 1 (NQO1) and manganese-containing superoxide dismutase (SOD2) on UC. NQO1 is an obligate two-electron reductase that catalyzes the reduction of quinines, quinine-imines, and nitro-compounds (Ross *et al.*, 2000). NQO1 may also play an antioxidant role via the reduction of endogenous quinones. The reduction of endogenous quinones helps to protect cellular membranes against oxidative damage.

SOD plays an important role in the protection of cells from the products of oxidative stress. SOD is an enzyme that catalyzes the dismutation of superoxide radicals to hydrogen

[1]Department of Internal Medicine, Second Teaching Hospital Fujita Health University School of Medicine, Nagoya, Japan.
[2]Medical Examination Center, Yachiyo Hospital, Anjou, Japan.
[3]Department of Pathologic Oncology, Mie University Graduate School of Medicine, Tsu, Japan.
[4]Inflammatory Bowel Disease Center and Department of Surgery, Yokkaichi Social Insulance Hospital, Yokkaichi, Japan.
[5]Department of Public Health, Graduate School of Medical Sciences, Kumamoto University, Kumamoto, Japan.
[6]Graduate School of Engineering, Yokohama National University, Yokohama, Japan.

peroxide. Two types of SOD lead to the requirement of the metal species at the active site: copper- and zinc-containing SOD (CuZn-SOD or SOD1, cytoplasmic) and manganese-containing SOD (Mn-SOD or SOD2, mitochondrial) (Crapo *et al.*, 1992; Guidot *et al.*, 1993). The other form is recently discovered. The forms containing Cu and Zn also have an extracellular (EC-SOD or SOD3) location (Zelko *et al.*, 2002). SOD2 is a mitochondrial enzyme that quenches free radicals and protects against oxidative stress by converting superoxide radicals to H2O2.

In this study, we conducted the study to investigate whether *NQO1* and *SOD2* polymorphisms influence the clinical characteristics of UC. In addition, the allele and genotype frequencies of the *NQO1* and *SOD2* polymorphisms were compared between UC patients and controls because of the possible influence these two polymorphisms might have on the incidence and clinical features of UC.

Materials and Methods

Subjects

We investigated 134 patients with UC (77 males and 57 females) and 125 healthy controls (67 males and 58 females). The UC patients were recruited between September 2004 and April 2007. The diagnosis of UC was based on conventional clinical, radiologic, endoscopic, and pathologic criteria. The characteristics of the UC patients are shown in Table 1. We analyzed the effect of *NQO1* and *SOD2* polymorphisms on the clinical characteristics. To assess the *NQO1* and *SOD2* polymorphisms in terms of influence on the incidence of UC, we compared the genotype frequencies of both polymorphisms in UC patients with those in controls.

Blood samples

Blood samples were collected from patients and controls after they had given informed consent to participate in this study. This study was approved by the Fujita Health University Ethics Committee. DNA was extracted from blood samples using a PUREGENE DNA isolation kit (Gentra Systems, Minneapolis, MN).

TABLE 1. CHARACTERISTICS OF PATIENTS WITH ULCERATIVE COLITIS

Age of onset (years)	36.7 ± 15.1
Colitis duration (years)	9.6 ± 7.8
Extension	
Proctitis	23 (17.2%)
Left-sided	58 (43.3%)
Pancolitis	53 (39.5%)
Type of clinical course	
First episode	16 (11.9%)
Chronic relapse	79 (59.0%)
Chronic persistent	39 (29.1%)
Severity	
Mild	40 (29.9%)
Moderate	60 (44.8%)
Severe	34 (25.3%)

The total number of patients with ulcerative colitis was 134. First episode, patients presenting with a first episode of colitis; chronic relapse, patients repeated relapse and remission; chronic persistent, patients continued active colitis over 6 months from first episode; severity is classified by Truelove and Witts' classification.

Genotypes

The *NQO1* C609T and *SOD2* Ala-9Val polymorphisms were recognized using polymerase chain reaction (PCR)–restriction fragment length polymorphisms. The primer sets were as follows (Olson *et al.*, 2004): for *NQO1*, 5′-ATTCTC TAGTGTGCCTGAG-3′ (forward) and 5′-AATCCTGCCTG GAAGTTTAG-3′ (reverse); for *SOD2*, 5′-ACCAGCAGGCA GCTGGCGCCGG-3′ (forward) and 5′-GCGTTGATGTGAG GTTCCAG-3′ (reverse). The PCR amplifications were performed in a 30-μL aliquot containing 50 ng of genomic DNA, 12 pmol of each primer, 3.0 μL of 10× buffer solution, 20 nmol/μL of dNTP, and 1 U of Taq polymerase. The PCR conditions for *NQO1* included an initial denaturation step at 95°C for 5 min, followed by 35 amplification cycles, each cycle containing denaturation at 95°C for 30 s, primer annealing at 60°C for 30 s, and extension at 72°C for 30 s, and then a final extension at 72°C for 7 min. PCR conditions for *SOD2* included an initial denaturation step at 95°C for 5 min, followed by 35 amplification cycles, each cycle containing denaturation at 95°C for 30 s, primer annealing at 63°C for 30 s, and extension at 72°C for 30 s, and then a final extension at 72°C for 7 min. The PCR products were subjected to overnight digestion with *Hin*fIV for *NQO1* at 37°C (Phillips *et al.*, 2004) and *Ngo*MIV for *SOD2* at 37°C (Akyol *et al.*, 2004) and then electrophoresed in 2% agarose gels. The digestion products gave the following band patterns: for *NQO1*, 318 bp for the wild-type C/C; 164 and 154 bp for the variant T/T; and 318, 164, and 154 bp for the heterozygous C/T (Fig. 1). For *SOD2*, the digestion products gave the following band patterns: 107 bp for the wild-type T/T; 89 and 18 bp for the variant C/C; 107, 89, and 18 bp for the heterozygous C/T (Fig. 2). Some of the digested *NQO1* and all of the *SOD2* products were examined on 12.5% polyacrylamide gels (Gene Gel Excel 12.5/24 kit from GE Healthcare Bio-Sciences, Tokyo, Japan) and stained with a DNA silver staining kit (GE Healthcare Bio-Sciences). The *NQO1* T/T genotype was expected to show two DNA bands of 164 and 154 bp; however, in this study, the T/T genotype resolved as a single band on an agarose gel. The two bands were clearly resolved on a polyacrylamide gel. The 164 and 154 bp bands showed a similar electrophoretic pattern for the C/T genotype. The band of 18 bp for the *SOD2* C/T and C/C genotypes was not clearly identified because the band was very small; however, the 107 and 89 bp bands were clearly recognized on a polyacrylamide gel. The results of PCR–restriction fragment length polymorphisms were confirmed by direct sequencing. DNA was extracted from the agarose gels using an extraction kit (Qiagen, Hilden, Germany). The genotypes were confirmed by sequence analysis using an auto sequencer (data not shown).

Statistical analysis

All data were analyzed by STATA10.0 (Stata Corporation, College Station, TX). The clinical features of UC, allele frequency, and genotype distribution were evaluated by a logistic regression test. Each polymorphism was tested to ensure that it did not deviate from Hardy–Weinberg equilibrium by the χ^2-test.

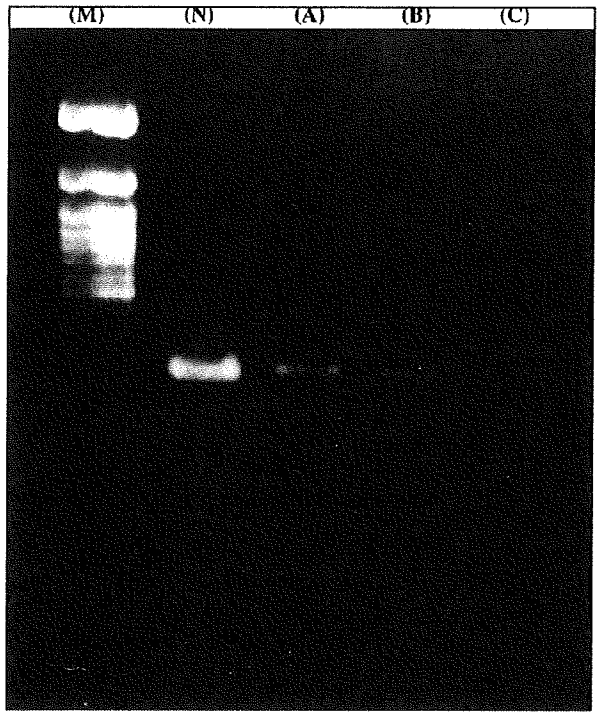

FIG. 1. Electrophoresed pattern of *NQO1* polymorphism. **(M)**, marker; **(N)**, no digestion (318 bp); **(A)**, C/C genotype (318 bp); **(B)**, C/T genotype (318 and 164 bp); **(C)**, T/T genotype (164 bp). This figure shows the electrophoresed pattern of *NQO1* polymorphisms on 2% agarose gel stained with ethidium bromide. **(A)** This pattern was identified to be 318 bp for C/C wild type. **(B)** This pattern was identified to be a heterozygous type for C/T. **(C)** This pattern was identified to be a variant type for T/T. The *NQO1* T/T band genotype was expected to show two DNA bands of 164 bp and 154 bp; however, in this study, the T/T genotype resolved as a single band on agarose gel. The two bands were clearly resolved on a polyacrylamide gel.

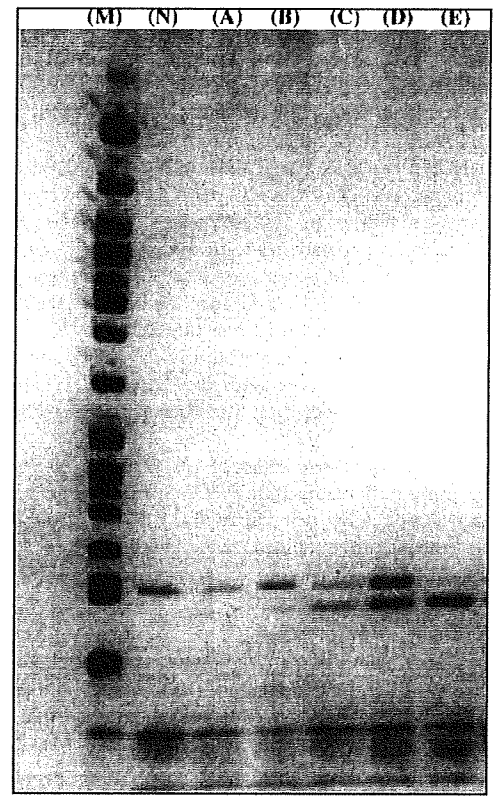

FIG. 2. Electrophoresed pattern of *SOD2* polymorphism on polyacrylamide gel. **(M)**, marker; **(N)**, no digestion (107 bp); **(A)** and **(B)**, T/T genotype (107 bp); **(C)** and **(D)**, C/T genotype (107 and 89 bp). **(E)**, C/C genotype (89 bp). This figure showed the electrophoresed pattern of *SOD2* polymorphism on 12.5% polyacrylamide gel. **(A)** and **(B)** are patterns that were identified to be wild type for T/T. **(C)** and **(D)** are patterns that were identified to be a heterozygous type for C/T. **(E)** is a pattern that was identified to be a variant type for C/C. The band of 18 bp for C/T and C/C genotypes was not clearly identified because the band was very small; however, the 107 and 89 bp bands were clearly recognized on a polyacrylamide gel.

Results

NQO1 *and* SOD2 *polymorphism genotypes*

The allele frequencies of the *NQO1* and *SOD2* polymorphisms and the genotype frequencies are shown in Table 2. Three control samples could not be genotyped for the *SOD2* polymorphism. The genotype data were consistent with the Hardy–Weinberg equilibrium (*NQO1*—patient group: $\chi^2 = 2.79$, $p = 0.10$; control group: $\chi^2 = 0.01$, $p = 0.90$) (*SOD2*—patient group: $\chi^2 = 1.82$, $p = 0.18$; control group: $\chi^2 = 3.59$, $p = 0.06$). In the control group, the frequencies of the C/C, C/T, and T/T genotypes for the *NQO1* polymorphism were 39.2%, 46.4%, and 14.4%, respectively, whereas the frequencies of the C/C, C/T, and T/T genotype for the *SOD2* polymorphism were 0.8%, 34.4%, and 64.8%, respectively. In the UC patients, the genotype and allele frequencies of neither the *NQO1* nor the *SOD2* polymorphisms differed significantly from the controls.

Influence of NQO1 *and* SOD2 *polymorphisms on the clinical characteristics of UC*

We attempted to identify an association between the *NQO1* and *SOD2* polymorphisms and the clinical features of

TABLE 2. GENOTYPE FREQUENCY OF NAD(P)H:QUINONE OXIDOREDUCTASE 1 AND SUPEROXIDE DISMUTASE

	UC (n = 134)/ *control* (n = 125)	*OR (95% CI)*	p
NQO1			
C/C/ + C/T	109/107	1.00 (referent)	
T/T	25/18	0.73 (0.37–1.42)	0.354
SOD2			
C/C + C/T	39/44[a]	1.00 (referent)	
T/T	95/78	0.73 (0.43–1.24)	0.243

The genotype frequency of *NQO1* and *SOD2* is compared between UC and control. In the UC patients, the genotype and allele frequencies of neither the *NQO1* nor the *SOD2* polymorphisms differed significantly from the controls.

[a]Three control samples could not be genotyped for *SOD2* polymorphism.

OR, odds ratio; CI, confidence interval; *NQO1*, NAD(P)H:quinone oxidoreductase 1; *SOD2*, superoxide dismutase.

the UC patients (age of onset, sex, nature of clinical course, severity of colitis, and steroid resistance). The severity of colitis was classified using the Truelove and Witts' classification (Truelove *et al.*, 1978). We defined the steroid-resistant group as patients who did not have remission with a conventional steroid dose, and required surgery or other therapy, such as plasma exchange. The association between the clinical characteristics of the UC patients and the two polymorphisms are shown in Tables 3 and 4. Regarding the severity of colitis, more patients with the *NQO1* T/T genotype developed severe colitis compared to the other genotypes (odds ratio [OR] 2.20, 95% confidence interval [CI] 0.69–6.95). In Table 5, the data of steroid resistance in the UC patients and the two polymorphisms are summarized. A significantly greater number of patients with the *NQO1* T/T genotype showed steroid resistance than the other genotypes (OR 9.20, 95% CI 2.19–38.7, $p = 0.002$).

For the patients whose onset of UC was age 20 years or younger, more patients had the *SOD2* T/T genotype than the other genotypes (OR 6.56, 95% CI 0.83–51.7, $p = 0.074$). Considering the other factors investigated, such as the severity of colitis, there was no difference in the *SOD2* polymorphisms among the patients.

Discussion

In this study, we investigated the association between polymorphisms related to oxidative stress and UC. The *NQO1* gene is located on 16q22 (Jaiswal, 1991). The *NQO1* C609T polymorphism encoded by codon 187 in exon 6 (Traver *et al.*, 1997) includes a single C-to-T substitution of the *NQO1* cDNA that causes a Pro187Ser amino acid change. This substitution leads to a reduction in the activity of the enzyme C/T heterozygotes and no activity in T/T homozygotes (Siegel *et al.*, 1999). The T allele of *NQO1* may be associated with an increased risk of various type of malignancy, including leukemia (Larson *et al.*, 1999; Naoe *et al.*, 2000), esophageal cancer (Zhang *et al.*, 2003), and colorectal cancer (Lafuente *et al.*, 2000).

TABLE 3. CLINICAL FEATURES OF ULCERATIVE COLITIS AND NAD(P)H:QUINONE OXIDOREDUCTASE 1 POLYMORPHISM

Clinical feature	NQO1 *genotype* C/C+ C/T/T/T	*OR (95% CI)*	p
Age			
<20	12/3	1.00 (referent)	
≥20	97/22	0.89 (0.23–3.46)	0.871
Sex			
Male	65/12	1.00 (referent)	
Female	44/13	1.55 (0.65–3.72)	0.329
Extension			
Proctititis	21/2	0.57 (0.11–2.95)	0.499
Left-sided	45/14	1.83 (0.68–5.04)	0.228
Pancolitis	43/8	1.00 (referent)	
Type of clinical course			
First episode	11/5	1.00 (referent)	
Chronic relapse	67/12	0.38 (0.11–1.34)	
Chronic persistent	31/8	0.56 (0.15–2.17)	0.321
Severity			
Mild	34/6	1.00 (referent)	
Moderate	51/9	0.93 (0.32–3.10)	
Severe	24/10	2.20 (0.75–7.51)	0.203

The table shows the relationship between clinical features of UC and *NQO1* genotype. Regarding the severity of colitis, more patients with the *NQO1* T/T genotype developed severe colitis compared to the other genotypes (OR 2.20).

TABLE 4. CLINICAL FEATURES OF ULCERATIVE COLITIS AND SUPEROXIDE DISMUTASE POLYMORPHISM

Clinical feature	SOD2 *genotype* T/T/C/C+C/T	*OR (95% CI)*	p
Age			
<20	14/1	1.00 (referent)	
≥20	81/38	6.56 (0.83–51.7)	0.074
Sex			
Male	56/22	1.00 (referent)	
Female	39/17	1.09 (0.51–2.31)	0.826
Extension			
Proctititis	15/7	0.95 (0.32–2.78)	0.925
Left-sided	45/14	0.58 (0.25–1.33)	0.197
Pancolitis	34/18	1.00 (referent)	
Type of clinical course			
First episode	11/5	1.00 (referent)	
Chronic relapse	26/14	0.75 (0.23–2.45)	
Chronic persistent	58/20	1.19 (0.34–4.15)	0.746
Severity			
Mild	27/11	1.00 (referent)	
Moderate	46/14	0.72 (0.29–1.83)	
Severe	22/14	1.50 (0.57–3.99)	0.489

The table shows the relationship between clinical features of UC and *SOD2* genotype. For the patients whose onset of UC was age 20 years or younger, a higher proportion had the *SOD2* T/T genotype than the other genotypes (OR 6.56, $p = 0.074$).

TABLE 5. STEROID RESISTANCE WITH ULCERATIVE COLITIS AND TWO POLYMORPHISMS

Steroid resistance	*Genotype*	*OR (95% CI)*	p
NQO1	C/C+C/T/T/T		
Steroid effective ($n = 65$)	58/7	1.00 (referent)	
Steroid resistance ($n = 18$)	11/7	9.20 (2.19–38.7)	0.002
SOD2	T/T/C/C+C/T		
Steroid effective ($n = 65$)	44/21	1.00 (referent)	
Steroid resistance ($n = 17$)	13/5	0.81 (0.25–2.61)	0.727

In this table, the data of steroid resistance in the UC patients and the two polymorphisms are summarized. A significantly greater number of patients with the *NQO1* T/T genotype showed steroid resistance than the other genotypes ($p = 0.002$).

The *SOD2* gene is located on 6q25 (Church *et al.*, 1992). The *SOD2* Ala-9Val polymorphism has a structural mutation of a T-to-C substitution in the coding sequence that changes the amino acid codon at the −9 position in the signal peptide from valine to alanine (Shimoda-Matsubayashi *et al.*, 1996). The C allele may confer an advantage to the SOD2 protein, rendering C/C genotype and C/T genotype than the T/T genotype (Sutton *et al.*, 2003). The Ala-9Val polymorphism has been associated with various diseases, such as Parkinson's disease (Shimoda-Matsubayashi *et al.*, 1996), nonfamilial idiopathic cardiomyopathy (Hiroi *et al.*, 1999), breast cancer (Ambroson *et al.*, 1999), and colorectal cancer (Stoehlmacher *et al.*, 2002).

This study provided two interesting findings of the *NQO1* polymorphism associated with UC. First, a significantly greater number of patients with the *NQO1* T/T genotype showed steroid resistance than the other genotypes. Second, more patients with the *NQO1* T/T genotype contracted severe colitis than the other genotypes. According to a previous report, the T/T genotype for *NQO1* C609T polymorphism has a null phenotype. NQO1 plays a role as a superoxide scavenger. Because of its role, NQO1 protects against superoxide-induced toxicity. Kruidenier *et al.* (2003) reported that intestinal inflammation was accompanied by excessive production of reactive metabolites. In addition, nitric oxide synthase and xanthine oxidase were both associated with oxidative stress in IBD. No studies have yet shown that NQO1 directly influences oxidative stress in IBD. However, patients with the *NQO1* T/T genotype may not prevent oxidative stress in the intestinal mucosa because the T/T genotype suppresses the activity of this enzyme. The suppression of NQO1 may influence the severity of UC.

The precise mechanism of steroid resistance in UC remains unclear. About 20–30% of the patients with severe acute UC make a poor response to corticosteroids (Hyde and Jewell, 1997). Involvement of genetic polymorphisms has been previously reported. Farrell and Kelleher (2003) reviewed glucocorticoid resistance in IBD. This review focused on the molecular mechanism of glucocorticoid resistance for the multidrug resistance gene (*MDR1*). The *MDR1* gene codes for a drug efflux pump, P-glycoprotein (Hoffmeyer *et al.*, 2000). MDR1 expression was elevated in UC and CD patients who required bowel resection for failed medical therapy (Farrell *et al.*, 2000). This suggests that IBD patients who failed to respond to medical therapy might escape effective immunosuppression by steroids and other immunosuppressive agents, because these drugs were MDR substrates and were pumped out of the target cells due to P-glycoprotein–mediated efflux. The association between *MDR1* polymorphism and cyclospoline A failure was investigated in patients with steroid resistant UC (Daniel *et al.*, 2007). The TT genotype in exon 21 of *MDR1* was associated with a higher risk of cyclospoline A failure in these patients.

Single-nucleotide polymorphisms of Solute Carrier Family (*SLC*) *22A4/5* have received greater clinical attention because they can modulate their transporter functions, causing individual variations in drug responsiveness (Newman *et al.*, 2005). In a Japanese study, the association of *SLC22A4/5* with steroid responsiveness of IBD was investigated (Nakahara *et al.*, 2008). The CG haplotype, comprising the C allele of the −446C > T and −368T > G in *SLC22A5* appeared to be a predictor of steroid resistance in Japanese patients with CD.

The previous report proposed that the criteria to predict patients with severe UC would respond poorly to intensive medical treatment and require colectomy (Travis *et al.*, 1996). According to the criteria, patients with frequent stools (>8/day), or raised C-reactive protein (CRP) levels (>450 mg/L) after 3 days of intensive treatment, need to be identified, as most will require colectomy on that admission. The criteria suggested that patients with severe UC applied to the criteria would respond poorly to intravenous corticosteroid therapy and require colectomy. Severe colitis of UC may induce steroid resistance (Esteve *et al.*, 2008). However, severe colitis does not necessarily resulted in steroid resistance; it is thought that severe colitis is assumption of steroid resistance.

Several factors cause steroid resistance, including oxidative stress. It has been reported that oxidative stress affected steroid resistance because of reduced Histone deacetylase 2 (HDAC-2) activity (Marwick *et al.*, 2007). Chromatin is subjected to a variety of posttranslational modifications known as the histone code that ultimately affect gene transcription. This modification such as acetylation and deacetylation are programmed by two families of enzymes referred to as histone acetyltransferases and HDACs. HDAC-2 plays a pivotal role in corticoid action, and recruits corticosteroid through the glucocorticoid receptor. Under condition of oxidative stress, HDAC-2 is inactivated and cannot be recruited into the corepressor by glucocorticoid receptor. This mechanism results in steroid resistance. Patients with *NQO1* T/T genotype have insufficient prevention of oxidative stress. The insufficient prevention of oxidative stress causes steroid resistance in patients with *NQO1* T/T genotype.

In the patients with an age of onset at age 20 years or younger, more had the *SOD2* T/T genotype than the other genotypes, suggesting that the T/T genotype might be associated with the age of onset of UC. As for the significance of the relatively early disease onset, the *SOD2* gene might influence the onset of disease directly or by acting upon another gene or factor. However, Taufer *et al.* (2005) showed that the *SOD2* polymorphism was associated with DNA damage in association with oxidative stress. These authors assumed that SOD2 supported the free radical theory of aging. Another author suggested that the T allele resulted in less effective targeting of SOD2 (Shimoda-Matsubayashi *et al.*, 1996). Our results may indicate that this genotype is associated with insufficient prevention of oxidative stress, and the resulting increase in oxidative stress may cause the development of colitis at a younger age.

In conclusion, the *NQO1* C609T polymorphism may influence the severity of UC and steroid resistance in UC patients, while the *SOD2* Ala-9Val polymorphism may influence the age at onset of UC. Further studies are needed to investigate the effect of *NQO1* and *SOD2* polymorphisms on UC.

Disclosure Statement

No competing financial interests exist.

References

Akyol, O., Canatan, H., Yilmaz, H.R., Yuce, H., Ozyurt, H., Sogut, S., Gulec, M., and Elyas, H. (2004). PCR/RFLP-based cost-effective identification of SOD2 signal (leader) sequence

polymorphism(Ala-9Val) using *Ngo*M IV: a detailed methodological approach. Clin Chim Acta **245,** 151–159.

Ambrosone, C.B., Freudebeim, J.L., Thompson, P.A., Bowman, E., Vena, J.E., Marshall, J.R., Graham, S., Laughlin, R., Nemoto, T., and Shields, P.G. (1999). Manganese superoxide dismutase (MnSOD) genetic polymorphisms, dietary antioxidants, and risk of breast cancer. Cancer Res **59,** 602–606.

Church, S.L., Grant, J.W., Meese, E.U., and Trent, J.M. (1992). Sublocalization of the gene encoding manganese superoxide dismutase (MnSOD/SOD2) to 6q25 by fluorescence *in situ* hybridization and somatic cell hybrid mapping. Genomics **14,** 823–825.

Crapo, J.D., Oury, T., Rabouille, C., Slot, J.W., and Chang, L.Y. (1992). Copper, zinc superoxide dismutase is primarily a cytosolic protein in human cells. Proc Natl Acad Sci USA **89,** 10405–10409.

Daniel, F., Loriot, M.A., Seksik, P., Cosnes, J., Gornet, J.M., Lémann, M., Fein, F., Vernier-Massouille, G., De Vos, M., Boureille, A., Treton, X., Flourie, B., Roblin, X., Louis, E., Zerbib, F., Beaune, P., and Marteau, P. (2007). Multidrug resistance gene-1 polymorphisms and resistance to cyclosporine A in patients with steroid resistant ulcerative colitis. Inflamm Bowel Dis **13,** 19–23.

Esteve, M., and Gisbert, J.P. (2008). Severe ulcerative colitis: at what point should we define resistance to steroids? World J Gastroenterol **14,** 5504–5507.

Farrell, R.J., and Kelleher, D. (2003). Mechanisms of steroid action and resistance in inflammation. Glucocorticoid resistance in inflammatory bowel disease. J Endocrinol **178,** 339–346.

Farrell, R.J., Murphy, A., Long, A., Donnelly, S., Cherikuri, A., O'Toole, D., Mahmud, N., Keeling, P.W., Weir, D.G., and Kelleher, D. (2000). High multidrug resistance (P-glycoprotein 170) expression in inflammatory bowel disease patients who fail medical therapy. Gastroenterology **118,** 279–288.

Guidot, D.M., McCord, J.M., Wright, R.M., and Repine, J.E. (1993). Absence of electron transport (Rho 0 state) restores growth of a manganese-superoxide dismutase-deficient *Saccharomyces cerevisiae* in hyperoxia: evidence for electron transport as a major source of superoxide generation *in vivo*. J Biol Chem **2678,** 26699–26703.

Hiroi, S., Harada, H., Nishi, H., Sato, M., Nagai, R., and Kimura, A. (1999). Polymorphisms in the SOD2 and HLA-DRB1 genes are associated with nonfamilial idiopathic dilated cardiomyopathy in Japanese. Biochem Biophys Res Commun **261,** 332–339.

Hoffmeyer, S., Burk, O., von Richter, O., Arnold, H.P., Brockmöller, J., Johne, A., Cascorbi, I., Gerloff, T., Roots, I., Eichelbaum, M., and Brinkmann, U. (2000). Functional polymorphisms of the human multidrug-resistance gene: multiple sequence variations and correlation of one allele with P-glycoprotein expression and activity *in vivo*. Proc Natl Acad Sci USA **97,** 3473–3478.

Hyde, G.M., and Jewell, D.P. (1997). The management of severe ulcerative colitis. Aliment Pharmacol Ther **11,** 419–424.

Jaiswal, A.K. (1991). Human NAD(P)H:quinone oxidoreductase (NQO1) gene structure and induction by dioxin. Biochemistry **30,** 10647–10653.

Koutroubakis, I.E., Malliaraki, N., Dimoulios, P.D., Karmiris, K., Castanas, E., and Kouroumalis, E.A. (2004). Decreased total and corrected antioxidant capacity in patients with inflammatory bowel disease. Dig Dis Sci **49,** 1433–1437.

Koutroubakis, I., Manousos, O.N., Meuwissen, S.G., and Pena, A.S. (1996). Environmental risk factors in inflammatory bowel disease. Hepatogastroentrerology **43,** 381–393.

Kruidenier, L., Kuiper, I., Lamers, C.B., and Verspaget, H.W. (2003). Intestinal oxidative damage in inflammatory bowel disease: semi-quantification, localization, and association with mucosal antioxidants. J Pathol **201,** 28–36.

Lafuente, M.J., Casterad, X., Trias, M., Ascaso, C., Molina, R., Ballesta, A., Zheng, S., Wiencke, J.K., and Lafuente, A. (2000). NAD(P)H:quinone oxidoreductase-dependent risk for colorectal cancer and its association with the presence of K-*ras* mutations in tumor. Carcinogenesis **21,** 1813–1819.

Larson, R.A., Wang, Y., Banerjee, M., Wiemels, J., Hartford, C., Le Beau, M.M., and Smith, M.T. (1999). Prevalence of the inactivating 609C → T polymorphism in the NAD(P)H:quinone oxidoreductase gene in patients with primary and therapy-related myeloid leukemia. Blood **94,** 803–807.

Marwick, J.A., Ito, K., Adcock, I.M., and Kirkham, P.A. (2007). Oxidative stress and steroid resistance in asthma and COPD: pharmacological manipulation of HDAC-2 as a therapeutic strategy. Expert Opin Ther Targets **11,** 745–755.

Nakahara, S., Arimura, Y., Saito, K., Goto, A., Motoya, S., Shinomura, Y., Miyamoto, A., and Imai, K. (2008). Association of SLC22A4/5 polymorphisms with steroid responsiveness of inflammatory bowel disease in inflammatory bowel disease in Japan. Dis Col Rec **51,** 598–603.

Naoe, T., Takeyama, K., Yokozawa, T., Kiyoi, H., Seto, M., Uike, N., Ino, T., Utsunomiya, A., Maruta, A., Jin-nai, I., Kamada, N., Kubota, Y., Nakamura, H., Shimazaki, C., Horiike, S., Kodera, Y., Saito, H., Ueda, R., Wiemels, J., and Ohno, R. (2000). Analysis of genetic polymorphism in *NQO1, GST-M1, GST-T1,* and *CYP3A4* in 469 Japanese patients with therapy-related leukemia/myelodysplastic syndrome and *de novo* acute myeloid leukemia. Clin Cancer Res **6,** 4091–4095.

Newman, B., Gu, X., Wintle, R., Cescon, D., Yazdanpanah, M., Liu, X., Peltekova, V., van Oene, M., Amos, C.I., and Siminovitch, K.A. (2005). A risk haplotype in the Solute Carrier Family 22A4/22A5 gene cluster influences phenotypic expression of Crohn's disease. Gastroenterology **128,** 260–269.

Olson, S.H., Carlson, M.D., Ostrer, H., Harlap, S., Stone, A., Winters, M., and Ambrosone, C.B. (2004). Genetic variants in *SOD2, MPO,* and *NQO1,* and risk of ovarian cancer. Gynecol Oncol **93,** 615–620.

Orchard, T.R., Satsangi, J., Van Heel, D., and Jewell, D.P. (2000). Genetics of inflammatory bowel disease: a reappraisal. Scand J Immunol **51,** 10–17.

Phillips, R.M., Basu, S., Brown, J.E., Flannigan, G.M., Loadman, P.M., Martin, S.W., Naylor, B., Puri, R., and Shah, T. (2004). Detection of (NAD(P)H:quinone oxidoreductase-1, EC1.6.99.2) 609C → T and 459C → T polymorphisms in formalin-fixed, paraffin-embedded human tumour tissue using PCR-RFLP. Int J Oncol **24,** 1005–1010.

Ross, D., Kepa, J.K., Winski, S.L., Beall, H.D., Anwar, A., and Siegel, D. (2000). NAD(P)H:quinone oxidoreductase 1 (NQO1): chemoprotection, bioactivation, gene regulation and genetic polymorphisms. Chem Biol Interact **129,** 77–97.

Shimoda-Matsubayashi, S., Matsumine, H., Kobayashi, T., Nakagawa-Hattori, Y., Shimizu, Y., and Mizuno, Y. (1996). Structural dimorphism in the mitochondrial targeting sequence in the human manganese superoxide dismutase gene. A predictive evidence for conformational change to influence mitochondrial transport and a study of allelic in Parkinson's disease. Biochem Biophys Res Commun **226,** 561–565.

Siegel, D., McGuinness, S.M., Winski, S.L., and Ross, D. (1999). Genotype-phenotype relationships in studies of a polymorphism in NAD(P)H:quinone oxidoreductase 1. Pharmacogenetics **9,** 113–121.

Silverberg, M.S., Cho, J.H., Rioux, J.D., McGovern, D.P., Wu, J., Annese, V., Achkar, J.P., Goyette, P., Scott, R., Xu, W.,

Barmada, M.M., Kiel, L., Daly, M.J., Abraham, C., Bayless, T.M., Bossa, F., Griffiths, A.M., Ippoliti, A.F., Lahaie, R.G., Latiano, A., Paré, P., Proctor, D.D., Regueiro, M.D., Steinhart, A.H., Targan, S.R., Schumm, L.P., Kistner, E.O., Lee, A.T., Gregersen, P.K., Rotter, J.I., Brant, S.R., Taylor, K.D., Roeder, K., and Duerr, R.H. (2009). Ulcerative colitis-risk loci on chromosomes 1p36 and 12q15 found by genome-wide association study. Nat Genet **41,** 216–220.

Stoehlmacher, J., Ingles, S.A., Park, D.J., Zhang, W., and Lenz, H.J. (2002). The -9Ala/-9Val polymorphism in the mitochondrial targeting sequence of the manganese superoxide dismutase gene (MnSOD) is associated with age among Hispanics with colorectal carcinoma. Oncol Rep **9,** 235–238.

Sutton, A., Khoury, H., Prip-Buus, C., Cepanec, C., Pessavre, D., and Deqoul, F. (2003). The Ala 16 Val genetic dimorphism modulates the import of human manganese super oxide dismutase in amyotrophic rat liver mitochondria. Pharmacogenetics **13,** 145–157.

Taufer, M., Peres, A., de Andrade, V.M., de Oliveira, G., Sá, G., do Canto, M.E.P., dos Santos, A.R., Bauer, M.E., and da Cruz, I.B.M. (2005). Is the Val16Ala manganese superoxide dismutase polymorphism with the aging process? J Gerontol **60,** 432–438.

Traver, R.D., Siegel, D., Beall, H.D., Phillips, R.M., Gibson, N.W., Franklin, W.A., and Ross, D. (1997). Characterization of a polymorphism in NAD(P)H:quinone oxidoreductase (DT-diaphorase). Br J Cancer **75,** 69–75.

Travis, S.P., Farrant, J.M., Ricketts, C., Nolan, D.J., Mortensen, N.M., Kettlewell, M.G., and Jewell, D.P. (1996). Predicting outcome in severe ulcerative colitis. Gut **38,** 905–910.

Truelove, S.C., Willoughby, C.P., Lee, E.G., and Ketlewell, M.G. (1978). Further experience in the treatment in the severe attacks of ulcerative colitis. Lancet **2,** 1086–1088.

Zelko, I.N., Mariani, T.J., and Folz, R.J. (2002). Superoxide dismutase multigene family: a comparison of the CuZn-SOD (SOD1), Mn-SOD (SOD2), and EC-SOD (SOD3) gene structures, evolution, and expression. Free Radic Biol Med **33,** 337–349.

Zhang, J.H., Li, Y., Wang, R., Geddert, H., Guo, W., Wen, D.G., Chen, Z.F., Wei, L.Z., Kuang, G., He, M., Zhang, L.W., Wu, M.L., and Wang, S.J. (2003). NQO1C609T polymorphism associated with esophageal cancer and gastric cardiac carcinoma in North China. World J Gastroenterol **9,** 1390–1393.

Address correspondence to:
Junji Yoshino, M.D.
Department of Internal Medicine
Second Teaching Hospital Fujita Health University
School of Medicine
3-6-10 Otobashi, Nakagawaku
Nagoya 454-8509
Japan

E-mail: jyoshino@fujita-hu.ac.jp

Received for publication February 25, 2009; received in revised form July 2, 2009; accepted July 2, 2009.

Experimental and Molecular Pathology 88 (2010) 90–95

Contents lists available at ScienceDirect

Experimental and Molecular Pathology

journal homepage: www.elsevier.com/locate/yexmp

RhoB enhances migration and MMP1 expression of prostate cancer DU145

Misao Yoneda [a], Yoshifumi S. Hirokawa [b,*], Atsuyuki Ohashi [b], Katsunori Uchida [b], Daisuke Kami [c], Masatoshi Watanabe [c], Toyoharu Yokoi [a], Taizo Shiraishi [b], Shinya Wakusawa [a]

[a] Department of Medical Technology, Nagoya University School of Health Sciences, 1-1-20 Minami, Daiko, Higashi-ku, Nagoya City, Aichi, Japan
[b] Department of Pathologic Oncology, Institute of Molecular and Experimental Medicine, Faculty of Medicine, Mie University Graduate School of Medicine, 2-174 Edobashi, Tsu, Mie 514-8507, Japan
[c] Laboratory for Medical Engineering, Division of Materials Science and Chemical Engineering, Graduate School of Engineering, Yokohama National University, Japan

ARTICLE INFO

Article history:
Received 27 March 2009
and in revised form 15 September 2009
Available online 24 September 2009

Keywords:
RhoB
GSK-3
MMP1
Prostate cancer

ABSTRACT

Rho family protein regulates variety of cellular functions as cytoskeletal organization, cell proliferation and apoptosis. In the present study, we demonstrate that RhoB-overexpressed prostate cancer cells showed an enhanced cell motility and the administration of the GSK-3 inhibitors inhibited this increase in migration. Among the extracellular matrix and adhesion-related molecules, MMP1 RNA expression was increased in RhoB-overexpressed cells, administration of MMP inhibitor suppressed the collagen gel invasion in these cells. This is the first report evaluating RhoB function and the downstream signaling events in prostate cancer cell. Our results indicate that RhoB promotes cell motility and invasion in a metastatic prostate cancer cell.

Introduction

Rho GTPase, RhoA, RhoB and RhoC regulate the organization of the cytoskeleton and cell motility (Wheeler and Ridley 2004). Among the Rho family of proteins, particular attention has been focused on RhoA, Rac1 and Cdc 42 since these molecules play central roles in cell migration through the regulation and formation of actin stress fiber, filopodia and lamellipodia, respectively (Ridley and Hall, 1992; Ridley et al., 1992; Kozma et al., 1995). The relevance of the subcellular RhoB localization at the endosome (Adamson et al., 1992), an RhoB function, is proposed to regulate membrane trafficking such as EGF receptor (Wherlock et al., 2004) and Src (Sandilands et al., 2004). In addition to its GTPase status, RhoB function is also influenced by the C terminal prenylated modification of either farnesylation or geranylgeranylation in apoptotic response, mitosis, tumor growth and actin organization (Liu et al., 2000; Moasser et al., 1998; Chen et al., 2000; Allal et al. 2002). The RhoB protein is induced by a variety of stimuli in vitro, including UV irradiation, cytokines and growth factors (Prendergast 2001). In vitro cancer model, RhoB overexpression, inhibits migration and invasion. RhoB suppresses melanoma metastasis in mouse xenograft model (Jiang et al., 2004). On the contrary, fibroblasts from RhoB knockout mice migrate less than the wild-type counterpart (Liu et al., 2001).

Processing and or degrading varieties of substrates in extracellular milieu, the matrix metalloproteinases (MMPs) play central roles in tissue remodeling, promoting cancer invasion and metastasis (Sternlicht and Werb 2001). MMP1 is associated with a poor prognosis of colon cancer (Murray et al., 1996), involved in the invasive potential of lung cancer (Schütz et al., 2002). The genetic variants of MMP1, that lead to a high protein expression, are epidemiologically linked with ovarian cancer, metastatic melanoma and lung cancer (Sternlicht and Werb 2001; Sauter et al., 2008).

In preliminary experiments, when a prostate cancer cell line DU145 was treated with reagents that promoted DNA demethylation and chromatin acetylation, RhoB RNA expression was stimulated to about ninety times the level of the untreated cells. Treating the same reagents of another prostate cancer cell line LNCap, RhoB expression was enhanced only about two times. Here we generated DU145 cell lines stably expressing RhoB and examined the effect of RhoB on cellular motility and invasion.

Materials and methods

Cell lines and reagents

The human RhoB cDNA was PCR amplified from the Clone Collection (Open Biosystems, EHS1001-7571211) and subcloned into the pcDNA3-HA vector. After introduction of the vector with or without the insert into the prostate cancer DU145 cell line, G418-selected clones were isolated. Up-regulation of the RhoB RNA/protein in these cells was confirmed. The SCADS inhibitor kit was generously supplied from Screening Committee of Anticancer Drugs supported by a Grant-in-Aid for Scientific Research on Priority Area "Cancer" from The Ministry of Education, Culture, Sports, Science and Technology, Japan. Two GSK-3 inhibitors, GSK-3 inhibitor IX (CalbioChem, 361550) and Indirubin-3′-monoxime-5-sulphonic acid (CalbioChem, 402085), were added to the culture at a final concentration of 10 μM.

* Corresponding author. Fax: +81 59 231 5210.
E-mail address: ultray2k@clin.medic.mie-u.ac.jp (Y.S. Hirokawa).

0014-4800/$ – see front matter © 2009 Elsevier Inc. All rights reserved.
doi:10.1016/j.yexmp.2009.09.010

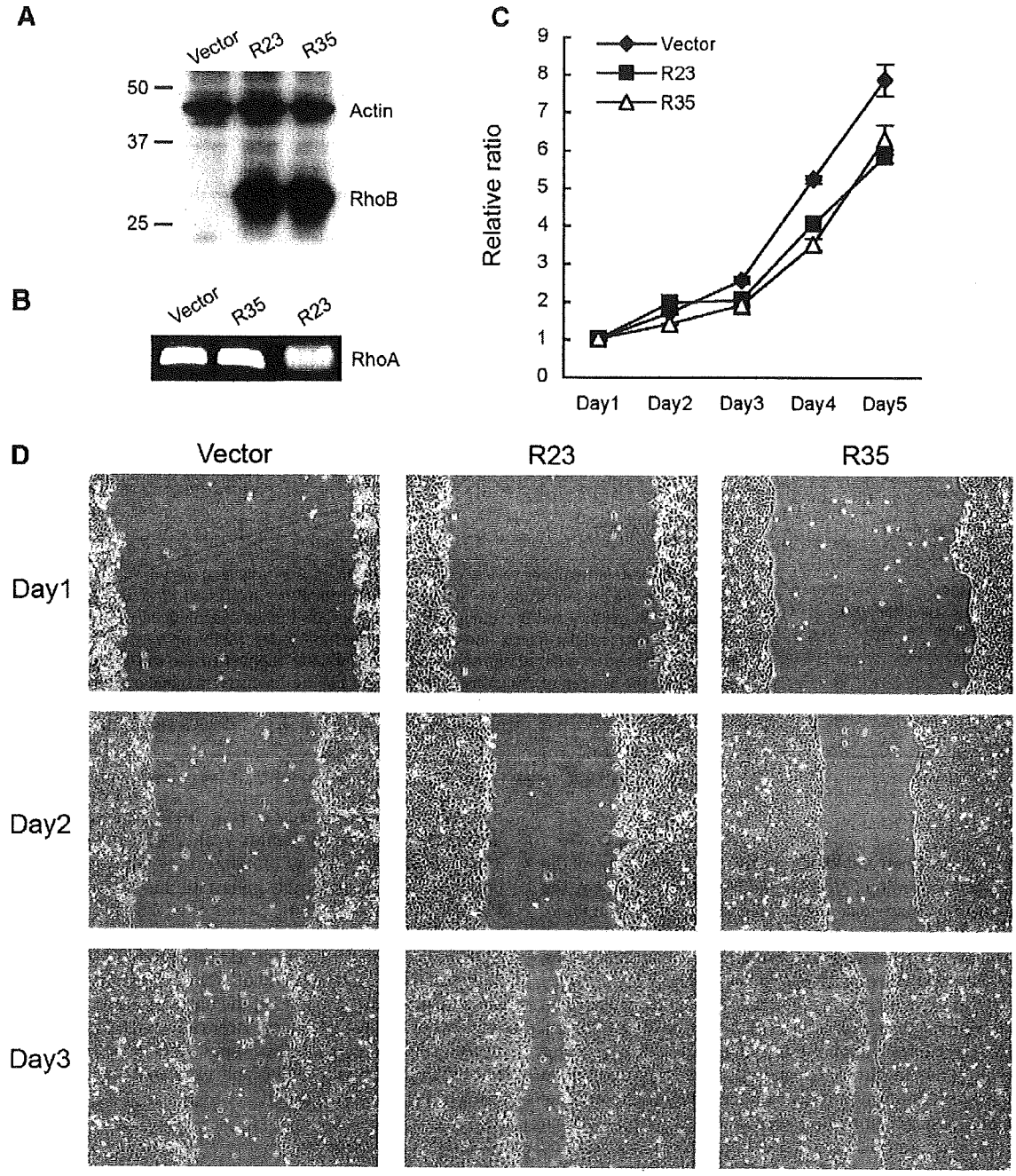

Fig. 1. RhoB overexpression promotes the migration of prostate cancer cells. (A) Western blot detection of two RhoB stably expressed clones R23 and R35 next to the vector-only-transfected clone. (B) RhoA mRNA expression levels in vector, R35 and R23 clone. (C) Cell growth up to 5 days culture are plotted as relative ratio to day 1. Data shown are mean ± SD of triplicates, representation from three independent experiments. (D) Wound closure assay with vector, R23 and R35 clones. Migration of each cell was observed for 3 days after the cells were scraped off. Images are representative of three independent experiments.

Wound closure/cell migration assays

The cells were cultured in RPMI 1640 (Sigma, R8758) with 10% fetal bovine serum (Gibco/Invitrogen) and seeded to a confluent density in 6 cm tissue culture dishes. For the wound closure assay, the monolayer of cells was scraped with the edge of a Cell Scraper (Iwaki, 9000-220). The cell migration assay was performed using the Boyden chamber method. Briefly, the cells were labeled with fluorescence DiI (Molecular Probes, D383) at 20 μg/ml in 6-cm tissue culture dishes for 6 h. DiI was dissolved in DMSO initially and then diluted in 100% EtOH. DiI-labeled 10^5 cells in 100-μl medium without FBS were loaded in the upper chamber (Falcon, 353097); the reagents from SCADS inhibitor kit and GSK-3 inhibitors were added to the bottom wells. After an overnight incubation, unmigrated cells were removed with a cotton swab, the chambers were placed in a new empty plate and the fluorescence of migrated cells was measured from the bottom direction using a plate reader.

The cell viability after administration of GSK-3 inhibitors was measured using the MTT assay according to the manufacturer's instructions (Promega, G3580). Each experiment was repeated at least twice in triplicate except for the SCADS inhibitor assay which was performed once because of the limited amount of the reagents.

Real-time PCR

Total RNA was isolated from prostate cancer cell lines using an RNA extraction kit according to the manufacturer's protocol (QIAGEN, 74104). First-strand cDNA synthesis was performed using the superscript II RNase Reverse Transcriptase kit (Invitrogen, 18080-044). The expression of 84 genes of the human extracellular matrix and adhesion molecules was analyzed according to the instructions of the RT^{2}Profiler PCR Array (SuperArray, PAHS-013A).

The primer sequences of RhoA were forward, 5′ TTACTCCGTAACA-GATTTTGTTGGC 3′, and reverse, 5′ ATACTACATCTAGTCTGGGGTAGAT 3′.

Collagen type I gel invasion assay

Invasion assays were carried out with a Cultrex 24-well collagen I cell invasion assay kit (3457-024-K) directed as the manufacture's instruction with a modification. Briefly, cells were cultured at 5×10^5 number in 6-cm plate, on the next day, 5×10^4 cells were suspended in 98 μl of RPMI 1640 with 0.5% fetal bovine serum, adding 2 μl of 5× collagen I solution, after mixing with pipeting, a 100-μl of cell/collagen mixed solution was aliquoted in each chamber (Falcon, 353097). Bottom well was loaded RPMI 1640 with 10% fetal bovine serum. After an overnight incubation, un-invaded cells were removed with a cotton swab, the chambers were placed back to the original wells with cell counting assay reagent (Cell Counting Kit-8, DOJINDO) and the absorbance of invaded cells was measured using a plate reader. Evaluating the MMP1 function of RhoB-overexpressed cells, MMP inhibitor II (CALBIOCHEM, #444247) was added to the medium of 6-cm plate at 100 μM and the cells were incubated for 6 h before the collagen gel chamber assay.

Both experiments were repeated three times in triplicate.

Results

RhoB overexpression enhanced prostate cancer cell migration

Two of the clones, designated R23 and R35, showed high RhoB protein expression compared to the vector-transfected clone (Fig. 1A). The proliferation rate at the culture conditions was slightly slower in R25 and R35 than vector-transfected cells, but this difference was not robust for the first three days (Fig. 1C). On culture days 4 and 5, vector-transfected cells grew faster than R25 and R35. Since RhoA also plays a pivotal role in cell proliferation, adhesion and migration, evaluating the RhoA status in prostate cancer cell migration under the test conditions was essential. The mRNA expression levels of RhoA were found to be similar in vector, R35 and R23 clone (Fig. 1B). When the migration rates were compared using the "wound closure assay", R23 and R35 showed faster movement than the vector clone in covering the "cellular defect" on the bottom of the scraped dish (Fig. 1D). This result clearly suggested the overexpression of the RhoB protein enhanced prostate cancer cell migration.

GSK-3 inhibitor suppressed migration of RhoB-expressed prostate cancer cells

In order to determine the signal mechanism underling the enhanced migration due to overexpression of the RhoB protein, an SCADS inhibitor kit was used for the migration assay. This kit includes several types of inhibitors commercially available. As described in the Materials and methods section, the initial cell migration was assessed by the Boyden chamber assay. Among the inhibitors inducing migratory suppression, GSK-3 inhibitors were chosen for the second round analysis. In cells treated with DMSO (vehicle), cell motility of R23 and R35 clones was twice that of the vector clone (Figs. 2A and B). Two of the GSK-3 inhibitors, GSK-3 inhibitor IX and Indirubin-3′-monoxime-5-sulphonic Acid, reduced the migration of R23 and R35 clones at the same level as that of the vector clone (Figs. 2A and B). Since the cell motility suppression was observed in the vector clone, GSK-3 inhibitors seemed to suppress endogenous RhoB effect as well. The cell viability of the three clones after treatment with GSK-3 inhibitors was not significantly different from each other (Fig. 2C).

Increased expression of MMP1 in RhoB-expressed prostate cancer and enhanced collagen gel invasion

Since cellular movement is closely associated with cell attachment, the mRNA levels of extracellular matrix and adhesion molecules were measured using real-time PCR (RT^{2}Profiler PCR Array). The most of gene expression levels were similar between R35 and vector clone (Table 1). The substantial fold changes between R35 versus vector clone were 2.36 of ADAM metallopeptidase with thrombospondin type 1 motif 8, 0.68 of E-cadherin, 0.55 of Vitronectin. Among the gene expression levels that were altered, MMP1 expression was about five times higher in the R35 clone than in the vector clone. The major substrates of MMP1 are collagens I, II and III. Verifying the functional relevance of MMP1 expression in the RhoB-overexpressed clones, chamber invasion assay was performed with type I collagen gel, which is the ubiquitously distributed interstitial matrix. Both R23 and R35 clones invaded through collagen gel more than vector clone (Fig. 3A). Prior to the chamber assay, incubating these cells with MMP inhibitor II, an inhibitor of MMP1, 3, 7 and 9, suppressed these enhanced cell invasion (Fig. 3B). These results indicate that MMP1 induction in RhoB-overexpressed prostate cancer cell is one of the mechanisms of increased migratory and invasive behavior of these cells.

Discussion

In the current study, we showed that the overexpression of RhoB enhanced cellular movement and invasion of prostate cancer cells in vitro. Increased motility is mediated by GSK-3 signaling and invasive potency is dependent on MMP1.

Previously, RhoB was shown to suppress the migration of NIH3T3 cells, invasion of pancreatic cancer cells and lung metastasis of melanoma cells (Jiang et al., 2004). RhoB-null macrophages also migrated faster on fibronectin (Wheeler and Ridley 2007). On the contrary, embryonic fibroblasts from an RhoB-null mouse showed less motility than wild-type fibroblasts in a wound closure test (Liu et al., 2001). Although the migratory mechanisms involved in these reverse functions of RhoB have not been fully elucidated yet, RhoB could play opposite roles within different cellular contexts. In NIH3T3 cells, GTPase-active and farnesylated RhoB can maintain an organized actin cytoskeleton and stress fibers against geranylgeranyl transferase inhibitor, which disrupts the actin cytoskeletal network (Allal et al., 2002). In this manner, the RhoB status of GTPase and prenylation could be different in each cellular type, consequently influencing actin fiber organization and cellular motility.

Fig. 2. GSK-3 inhibitors suppress motility of each cell clone in the chamber mobility assay. (A) Fluorescence microscope images of chamber membranes. Cells were plated inside the chamber in serum-free medium and allowed to migrate to serum and inhibitor-containing medium at the bottom for 12 h. (B) Migrated cell numbers were assessed in terms of the fluorescence value of each chamber. Data shown are mean ± SD of triplicates, representation from three independent experiments. (C) Cell viability of each clone was measured using the MTT assay after treatment of cells with GSK-3 inhibitors. Data shown are mean ± SD of triplicates, representation from two independent experiments.

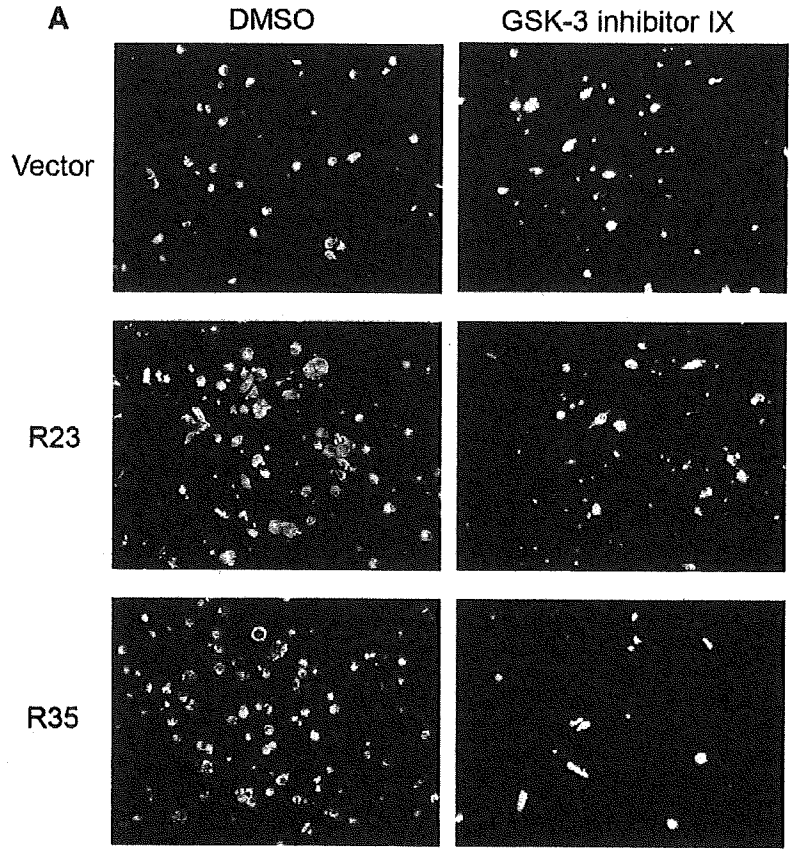
A
DMSO
GSK-3 inhibitor IX
Vector
R23
R35

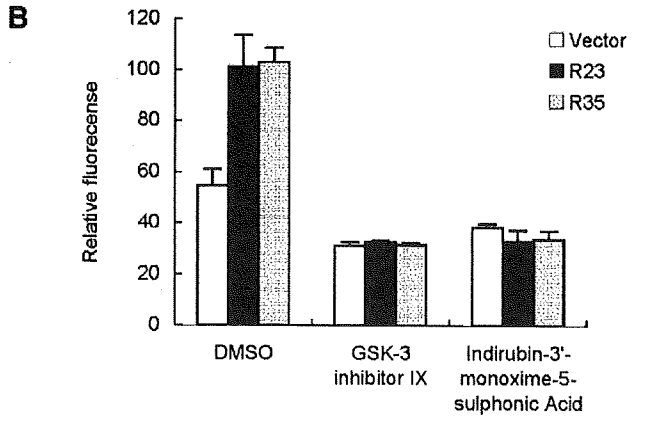
B
Relative fluorecense
120
100
80
60
40
20
0
Vector
R23
R35
DMSO
GSK-3 inhibitor IX
Indirubin-3'-monoxime-5-sulphonic Acid

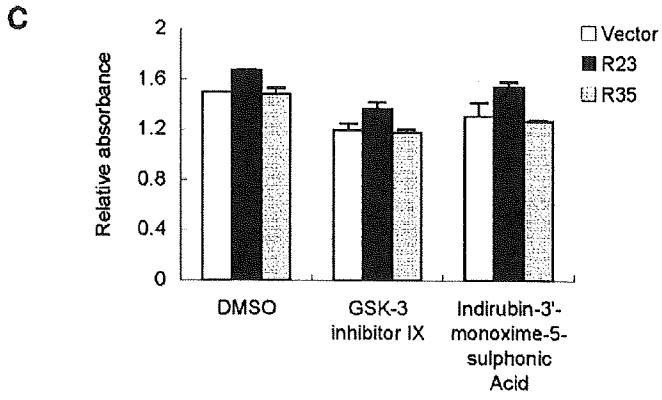
C
Relative absorbance
2
1.6
1.2
0.8
0.4
0
Vector
R23
R35
DMSO
GSK-3 inhibitor IX
Indirubin-3'-monoxime-5-sulphonic Acid

Table 1
Real-time PCR analysis of human extracellular matrix and adhesion molecules.

Gene	Fold change
ADAM metallopeptidase with thrombospondin type 1 motif, 1	1.03
ADAM metallopeptidase with thrombospondin type 1 motif, 13	0.96
ADAM metallopeptidase with thrombospondin type 1 motif, 8	2.36
CD44 molecule	1.18
Cadherin 1, E-cadherin	0.68
Contactin 1	0.84
Collagen, type XI, alpha 1	1.03
Collagen, type XII, alpha 1	0.39
Collagen, type XIV, alpha 1	1.03
Collagen, type XV, alpha 1	1.45
Collagen, type XVI, alpha 1	1.03
Collagen, type I, alpha 1	1.03
Collagen, type IV, alpha 2	1.92
Collagen, type V, alpha 1	1.03
Collagen, type VI, alpha 1	0.63
Collagen, type VI, alpha 2	0.73
Collagen, type VII, alpha 1	1.03
Collagen, type VIII, alpha 1	1.03
Versican	1.03
Connective tissue growth factor	0.63
Catenin, alpha 1	0.78
Catenin, beta 1	0.84
Catenin, delta 1	0.9
Catenin, delta 2	1.03
Extracellular matrix protein 1	1.67
Fibronectin 1	1.36
Hyaluronan synthase 1	1.03
Intercellular adhesion molecule 1 (CD54)	0.73
Integrin, alpha 1	1.18
Integrin, alpha 2 (CD49B)	1.56
Integrin, alpha 3 (antigen CD49C)	1.27
Integrin, alpha 4 (antigen CD49D)	1.03
Integrin, alpha 5 (fibronectin receptor)	0.73
Integrin, alpha 6	0.96
Integrin, alpha 7	1.03
Integrin, alpha 8	1.03
Integrin, alpha L (antigen CD11A)	1.03
Integrin, alpha M	1.03
Integrin, alpha V (vitronectin receptor)	1.1
Integrin, beta 1 (fibronectin receptor)	0.84
Integrin, beta 2	0.84
Integrin, beta 3 (antigen CD61)	1.03
Integrin, beta 4	1.67
Integrin, beta 5	1.03
Kallmann syndrome 1 sequence	1.03
Laminin, alpha 1	1.1
Laminin, alpha 2 (merosin)	1.03
Laminin, alpha 3	1.03
Laminin, beta 1	1.27
Laminin, beta 3	0.9
Laminin, gamma 1	0.78
Matrix metallopeptidase 1	5.06
Matrix metallopeptidase 10 (stromelysin 2)	1.03
Matrix metallopeptidase 11 (stromelysin 3)	0.78
Matrix metallopeptidase 12	1.03
Matrix metallopeptidase 13 (collagenase 3)	1.03
Matrix metallopeptidase 14	1.79
Matrix metallopeptidase 15	0.59
Matrix metallopeptidase 16	1.03
Matrix metallopeptidase 2	1.03
Matrix metallopeptidase 3 (stromelysin 1)	1.03
Matrix metallopeptidase 7 (matrilysin)	1.03
Matrix metallopeptidase 8	1.03
Matrix metallopeptidase 9	0.9
Neural cell adhesion molecule 1	1.03
Platelet/endothelial cell adhesion molecule (CD31 antigen)	1.03
Selectin E	1.03
Selectin L	0.84
Selectin P (antigen CD62)	1.03
Sarcoglycan, epsilon	0.84
Osteonectin	1.03
Spastic paraplegia 7	1.18
Secreted phosphoprotein 1 (osteopontin)	1.03
Transforming growth factor-beta	1.1
Thrombospondin 1	1.18
Thrombospondin 2	1.03
Thrombospondin 3	0.9
TIMP metallopeptidase inhibitor 1	1.67
TIMP metallopeptidase inhibitor 2	0.96
TIMP metallopeptidase inhibitor 3	1.03
C-type lectin domain family 3, member B	1.03
Tenascin C	1.79
Vascular cell adhesion molecule 1	1.03
Vitronectin	0.55
Beta-2-microglobulin	1.45
Hypoxanthine phosphoribosyltransferase 1	1.1

Fold changes of R35 to Vector clone were calculated according to the instructions of the RT^{2}Profiler PCR Array.

Because our data indicate that the GSK-3 inhibitors tested abrogated prostate cancer cell migration to the basal level, GSK-3 is postulated to play a pivotal role in cell motility under the RhoB-involved signal cascade. The role of RhoB in GSK-3 signaling has already been demonstrated under hypoxic conditions (Skuli et al., 2006). Hypoxic signals induced RhoB-dependent Akt and GSK-3 phosphorylation. An RhoB-overexpressed R35 cell line did not show predominantly phosphorylated Akt (Thr308 and Ser473, data not shown); thus, signal transduction to GSK-3 might bypass Akt activation in this cell line.

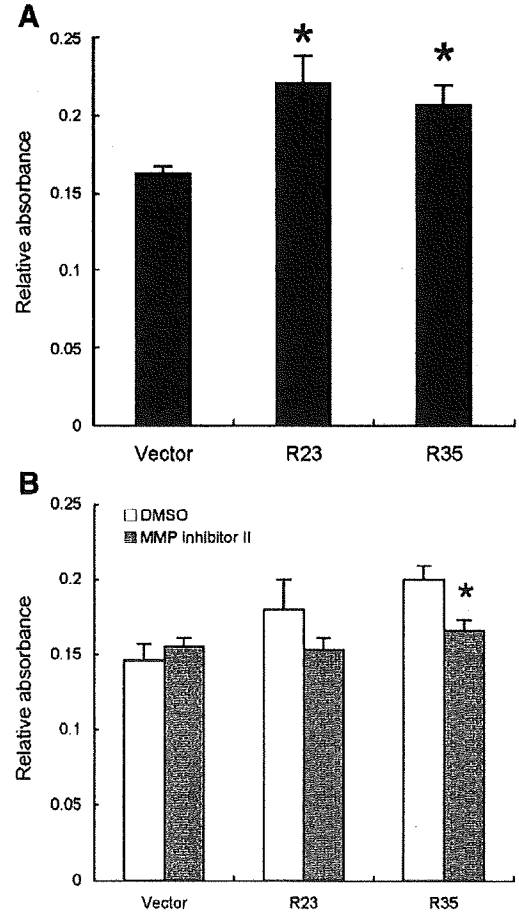

Fig. 3. Collagen gel invasion assays with or without MMP inhibitor. (A) Invasive potential of each clones were measured with Boyden chamber based assay system. Data shown are mean ± SD of triplicates, representation from three independent experiments. *$p<0.05$, compared to vector control. (B) Same collagen gel invasion assay in panel A, except each cells were pretreated with MMP inhibitor. Data shown are mean ± SD of triplicates, representation from three independent experiments. *$p<0.05$, compared to R35 DMSO. Mann–Whitney U-test was used to calculate statistical significances in panels A and B.

In addition to our current result, direct evidence showing that GSK-3 up-regulates epithelial cell migration has been presented using an MDCK wound closure assay (Farooqui et al., 2006). GSK-3 acts upstream of ADP-ribosylation factor 6 and Rac1, and the activated form of GSK-3 predominates during wound closure. The epithelial cell migration was blocked by an administration of GSK-3 inhibitor. The authors postulate that cell adhesion protein paxillin could be the downstream effecter molecule of GSK-3. Paxillin, which is a focal adhesion-associated protein, acts as a scaffold protein influencing cell motility and providing a signaling platform at the vicinity of focal adhesion (Brown and Turner, 2004). Since the phosphorylation of paxillin, which is essential in cell spreading, is mediated by GSK-3 and ERK dual-kinase (Cai et al., 2006), the phosphorylation levels of both proteins were evaluated in the R35 cell line. There was no difference in the phosphorylation status of GSK-3α (Ser21), GSK-3β (Ser9) and paxillin (Ser126) between R35 and vector cell lines (data not shown). GSK-3 phosphorylates target proteins preferably activated by other kinases (Doble and Woodgett, 2003). R35 and vector cells might have a different co-modifying set of kinases that target cell motile regulatory proteins.

Given the functional diversity, GSK-3 has been studied as a therapeutic target in many pathological conditions (Doble and Woodgett, 2003). Clinical and in vitro effects of GSK-3 inhibitors are insulin mimetic action, anti-cell proliferation and inhibition of tau phosphorylation. Recent studies have shown that administration of a GSK-3 inhibitor increased bone formation (Kulkarni et al., 2007) and prevented epithelial-mesenchymal transition (EMT) of human embryonic stem cell (Ullmann et al., 2008). EMT is the process of cytoskeletal and adhesion molecules to remodel an epithelial into mesenchymal phenotype, losing an original polarity but gaining a higher motility. Thus, close association of EMT with cancer invasion and metastasis, targeting GSK-3 by specific inhibitor, like our study and others, could become a therapeutic options for an advanced cancer.

The underlying mechanism between RhoB and MMP1 expression has not yet been fully elucidated. The cytoplasmic tail of a transmembrane mucin, MUC1, translocates to the nucleus after phosphorylation by Met, interacts with p53 and leads to the suppression of MMP1 transcription (Singh et al., 2008). MUC1 is also phosphorylated by GSK-3β (Li et al., 1998). The phosphorylation sites of MUC1 by Met and GSK-3β are not identical. So it is plausible that MUC1 in RhoB-overexpressed prostate cancer cells might be predominantly phosphorylated by GSK-3β, abrogating its suppressive effect on MMP1 transcription.

In the literature, there have been no solid data studying the relevance of RhoB and clinical cancer. One can assume that no correlation has been observed between clinical cancer and RhoB expression level. We did the compared real-time PCR experiment of RhoB in the cancer versus non-cancerous tissue from clinically dissected prostate cancer. The RhoB expression ratio (cancer/non-cancer) was diverse among each cancer cases and no correlation was observed toward Gleason score, an indicator of malignant potency and prognosis (data not shown). Based on the origin of DU145 cell line, which was derived from brain metastasis lesion, RhoB function as an invasion promoter might be exerted at distant metastatic prostate cancer. Even in this scenario, DNA demethylated and/or chromatin acetylated modification could be required for an induction of RhoB protein in prostate cancer cells as in our preliminary experiment.

In conclusion, this study presents the first evidence that RhoB promotes cellular motility and invasion of prostate cancer cell, signaling downstream in GSK-3 and enhancing a collagen gel invasion by MMP1 induction. Current results indicate that in certain cell type, like prostate cancer, RhoB works as a tumor promoter not as a suppressor. Unraveling the cell-type-specific bifunctional mechanisms and conditions of RhoB protein should help understanding the biological, physiological and pathological protein behavior.

References

Adamson, P., Paterson, H.F., Hall, A., 1992. Intracellular localization of the P21rho proteins. J. Cell Biol. 119, 617–627.

Allal, C., Pradines, A., Hamilton, A.D., Sebti, S.M., Favre, G., 2002. Farnesylated RhoB prevents cell cycle arrest and actin cytoskeleton disruption caused by the geranylgeranyltransferase I inhibitor GGTI-298. Cell Cycle 1, 430–437.

Brown, M.C., Turner, C.E., 2004. Paxillin adapting to change. Physiol. Rev. 84, 1315–1339.

Cai, X., Li, M., Vrana, J., Schaller, M.D., 2006. Glycogen synthase kinase 3- and extracellular signal-regulated kinase-dependent phosphorylation of paxillin regulates cytoskeletal rearrangement. Mol. Cell Biol. 26, 2857–2868.

Chen, Z., Sun, J., Pradines, A., Favre, G., Adnane, J., Sebti, S.M., 2000. Both farnesylated and geranylgeranylated RhoB inhibit malignant transformation and suppress human tumor growth in nude mice. J. Biol. Chem. 275, 17974–17978.

Doble, B.W., Woodgett, J.R., 2003. GSK-3: tricks of the trade for a multi-tasking kinase. J. Cell Sci. 116 (Part 7), 1175–1186.

Farooqui, R., Zhu, S., Fenteany, G., 2006. Glycogen synthase kinase-3 acts upstream of ADP-ribosylation factor 6 and Rac1 to regulate epithelial cell migration. Exp. Cell Res. 312, 1514–1525.

Jiang, K., Sun, J., Cheng, J., Djeu, J.Y., Wei, S., Sebti, S., 2004. Akt mediates Ras downregulation of RhoB, a suppressor of transformation, invasion, and metastasis. Mol. Cell. Biol. 24, 5565–5576.

Kozma, R., Ahmed, S., Best, A., Lim, L., 1995. The Ras-related protein Cdc42Hs and bradykinin promote formation of peripheral actin microspikes and filopodia in Swiss 3T3 fibroblasts. Mol. Cell. Biol. 15, 1942–1952.

Kulkarni, N.H., Wei, T., Kumar, A., Dow, E.R., Stewart, T.R., Shou, J., N'cho, M., Sterchi, D.L., Gitter, B.D., Higgs, R.E., Halladay, D.L., Engler, T.A., Martin, T.J., Bryant, H.U., Ma, Y.L., Onyia, J.E., 2007. Changes in osteoblast, chondrocyte, and adipocyte lineages mediate the bone anabolic actions of PTH and small molecule GSK-3 inhibitor. J. Cell Biochem. 102, 1504–1518.

Li, Y., Bharti, A., Chen, D., Gong, J., Kufe, D., 1998. Interaction of glycogen synthase kinase 3beta with the DF3/MUC1 carcinoma-associated antigen and beta-catenin. Mol. Cell. Biol. 18, 7216–7224.

Liu, A., Du, W., Liu, J.P., Jessell, T.M., Prendergast, G.C., 2000. RhoB alteration is necessary for apoptotic and antineoplastic responses to farnesyltransferase inhibitors. Mol. Cell. Biol. 20, 6105–6113.

Liu, A.X., Rane, N., Liu, J.P., Prendergast, G.C., 2001. RhoB is dispensable for mouse development but it modifies susceptibility to tumor formation as well as cell adhesion and growth factor signaling in transformed cells. Mol. Cell. Biol. 20, 6906–6912.

Moasser, M.M., Sepp-Lorenzino, L., Kohl, N.E., Oliff, A., Balog, A., Su, D.S., Danishefsky, S.J., Rosen, N., 1998. Farnesyl transferase inhibitors cause enhanced mitotic sensitivity to taxol and epothilones. Proc. Natl. Acad. Sci. U. S. A. 95, 1369–1374.

Murray, G.I., Duncan, M.E., O'Neil, P., Melvin, W.T., Fothergill, J.E., 1996. Matrix metalloproteinase-1 is associated with poor prognosis in colorectal cancer. Nat. Med. 2, 461–462.

Prendergast, G.C., 2001. Actin' up RhoB in cancer and apoptosis. Nat. Rev. Cancer 1, 162–168.

Ridley, A.J., Hall, A., 1992. The small GTP-binding protein rho regulates the assembly of focal adhesions and actin stress fibers in response to growth factors. Cell 70, 389–399.

Ridley, A.J., Paterson, H.F., Johnston, C.L., Diekmann, D., Hall, A., 1992. The small GTP-binding protein rac regulates growth factor-induced membrane ruffling. Cell 70, 401–410.

Sandilands, E., Cans, C., Fincham, V.J., Brunton, V.G., Mellor, H., Prendergast, G.C., Norman, J.C., Superti-Furga, G., Frame, M.C., 2004. RhoB and actin polymerization coordinate Src activation with endosome-mediated delivery to the membrane. Dev. Cell 7, 855–869.

Sauter, W., Rosenberger, A., Beckmann, L., Kropp, S., Mittelstrass, K., Timofeeva, M., Wölke, G., Steinwachs, A., Scheiner, D., Meese, E., Sybrecht, G., Kronenberg, F., Dienemann, H., Chang-Claude, J, Illig, T., Wichmann, H.E., Bickeböller, H., Risch, A., LUCY-Consortium, 2008. Matrix metalloproteinase 1 (MMP1) is associated with early-onset lung cancer. Cancer Epidemiol. Biomarkers Prev. 17, 1127–1135.

Schütz, A., Schneidenbach, D., Aust, G., Tannapfel, A., Steinert, M., Wittekind, C., 2002. Differential expression and activity status of MMP-1, MMP-2 and MMP-9 in tumor and stromal cells of squamous cell carcinomas of the lung,. Tumour. Biol. 23, 179–184.

Singh, P.K., Behrens, M.E., Eggers, J.P., Cerny, R.L., Bailey, J.M., Shanmugam, K., Gendler, S.J., Bennett, E.P., Hollingsworth, M.A., 2008. Phosphorylation of MUC1 by Met modulates interaction with p53 and MMP1 expression. J. Biol. Chem. 283, 26985–26995.

Skuli, N., Monferran, S., Delmas, C., Lajoie-Mazenc, I., Favre, G., Toulas, C., Cohen-Jonathan-Moyal, E., 2006. Activation of RhoB by hypoxia controls hypoxia-inducible factor-1alpha stabilization through glycogen synthase kinase-3 in U87 glioblastoma cells. Cancer Res. 66, 482–489.

Sternlicht, M.D., Werb, Z., 2001. How matrix metalloproteinases regulate cell behavior. Annu. Rev. Cell Dev. Biol. 17, 463–516.

Ullmann, U., Gilles, C., De Rycke, M., Van de Velde, H., Sermon, K., Liebaers, I., 2008. GSK-3-specific inhibitor-supplemented hESC medium prevents the epithelial–mesenchymal transition process and the up-regulation of matrix metalloproteinases in hESCs cultured in feeder-free conditions. Mol. Hum. Reprod. 14, 169–179.

Wheeler, A.P., Ridley, A.J., 2004. Why three Rho proteins? RhoA, RhoB, RhoC, and cell motility. Exp. Cell Res. 301, 43–49.

Wheeler, A.P., Ridley, A.J., 2007. RhoB affects macrophage adhesion, integrin expression and migration. Exp. Cell Res. 313, 3505–3516.

Wherlock, M., Gampel, A., Futter, C., Mellor, H., 2004. Farnesyltransferase inhibitors disrupt EGF receptor traffic through modulation of the RhoB GTPase. J. Cell Sci. 117 (Part 15), 3221–3231.

Elevated levels of 4-hydroxynonenal-histidine Michael adduct in the hippocampi of patients with Alzheimer's disease

Mitsugu Fukuda[1], Fumihisa Kanou[2], Nobuko Shimada[1], Motoji Sawabe[3], Yuko Saito[3,4], Shigeo Murayama[4], Masakatsu Hashimoto[2], Naoki Maruyama[1] and Akihito Ishigami[1,5]

[1]Aging Regulation, Tokyo Metropolitan Institute of Gerontology, Tokyo, Japan, [2]Shima Laboratories, Tokyo, Japan, [3]Department of Pathology, Tokyo Metropolitan Geriatric Hospital, Tokyo, Japan, [4]Department of Neuropathology, Tokyo Metropolitan Institute of Gerontology, Tokyo, Japan and [5]Department of Biochemistry, Faculty of Pharmaceutical Sciences, Toho University, Chiba, Japan

Address correspondence to: Akihito Ishigami, Ph.D. Department of Biochemistry, Faculty of Pharmaceutical Sciences, Toho University, Miyama 2-2-1, Funabashi, Chiba 274-8510, Japan. Phone/FAX: +81-47-472-1536, E-mail: ishigami@phar.toho-u.ac.jp

Running title : HNE adduct in Alzheimer's disease brain

Abbreviations used: AD, Alzheimer's disease; DAB, 3,3'-diaminobenzidine tetrahydrochloride; HNE, 4-hydroxynonenal; MAP2, microtubule-associated protein 2; NFT, neurofibrillary tangle; PBS, phosphate buffered saline; PUFAs, polyunsaturated fatty acids.

ABSTRACT

Alzheimer's disease (AD) is among the most common causes of progressive cognitive impairment in humans and is characterized by neurodegeneration in the brain. Lipid peroxidation is thought to play a role in the pathogenesis of AD. 4-hydroxynonenal (HNE) results from peroxidation of polyunsaturated fatty acids and it in turn gives evidence of lipid peroxidation *in vivo*. HNE reacts with protein histidine residue to form a stable HNE-histidine Michael adduct. To clarify the influence of lipid peroxidation on the pathogenesis of AD, we measured HNE-histidine Michael adduct in hippocampi from four AD patients and four age-matched controls by means of semiquantitative immunohistochemistry using a specific antibody to cyclic hemiacetal type of HNE-histidine Michael adduct. This antibody does not react with the ring-opened form of HNE-histidine Michael adduct and the pyrrole form of HNE-lysine Michael adduct. The HNE adduct was detected in the hippocampi of both AD and control donors, especially in the CA2, CA3 and CA4 sectors. Immunoreactive intensity of HNE adduct in these sectors were significantly higher in AD patients than in the controls. The HNE adduct was found in the perikarya of pyramidal cells in the hippocampus. These results show that the hippocampi of patients with AD undergo lipid peroxidation and imply that this activity underlies the production of cytotoxic products such as HNE that are responsible for the pathogenesis of AD.

INTRODUCTION

The progressive cognitive impairment of Alzheimer's disease (AD) is associated with neuronal loss as well as the formation of neurofibrillary tangles (NFTs) and senile plaques in the brain (25). Free radical-mediated oxidative damage, energy depletion, deposition of amyloids and NFTs, excitotoxicity, and vascular endothelial cell damage are all thought to participate in the pathogenesis of AD (13). Oxygen-derived free radicals, byproducts of respiration, cause oxidative damage to cellular biomolecules including lipids, proteins and nucleic acids. The brain seems to be especially vulnerable to lipid peroxidation by free radicals, because it consumes approximately one-fifth of humans' oxygen intake, has a relative paucity of antioxidant systems and contains high concentrations of polyunsaturated fatty acids (PUFAs) (11). Lipid peroxidation results in structural damage to membranes and generation of secondary products such as reactive aldehydes that modify proteins and nucleic acids (5). Therefore, as reported, lipid peroxidation in the brains of AD patients not only harms cells but increases levels of such peroxidation products as thiobarbituric acid-reactive substances (10), acrolein-deoxyguanosine adducts (9) and cytotoxic compounds such as acrolein (12) and 4-hydroxynonenal (HNE) (17).

Lipid peroxidation propagates itself by autoxidation initiated by free radicals and produces considerable amounts of secondary products before the process terminates (21). These well-known secondary products include reactive aldehydes, such as acrolein, malondialdehyde, HNE, and 4-hydroxyhexenal (5). HNE is product that results from the lipid peroxidation of n-6 PUFAs, e.g., linoleic acid and arachidonic acid (5). Because the brain is rich in arachidonic acid (29), lipid peroxidation tends to produce HNE at that site. These substances then react with proteins, nucleic acids and small molecules such as glutathione in cells and eventually impair normal biological functions of the essential components (5). Indeed, HNE is cytotoxic for cultured neuronal cells (2, 5, 8, 15). Therefore, HNE might induce neuronal cell death and neurodegeneration in patients with AD.

Measuring the exact quantity of HNE *in vivo* is difficult, since they are rapidly consumed when their chemically active aldehyde reacts with such cellular components as glutathione, proteins and nucleic acids (5). HNE react with lysine, histidine and cysteine residues in proteins to form Michael adducts and also Schiff base products (lysine ε-NH_2). When HNE reacts with proteins, HNE-histidine Michael adduct is a major product that develops in the